UNIVERSITY OF CALIFORNIA SAN DIEGO

Functional Tug of War between Hog1 and Gcn5-PP2A^{Rts1} at the Spindle Assembly Check Point

A thesis submitted in partial satisfaction of the requirements
for the degree Master of Science

in

Biology

by

Qihao Liu

Committee in charge:

Professor Lorraine Pillus, Chair
Professor Nan Hao
Professor James Kadonaga

2022

The thesis of Qihao Liu is approved, and it is acceptable in quality and form for publication on microfilm and electronically.

University of California San Diego

2022

DEDICATION

This thesis is a dedication to the three families I fortunately encountered in this life

To my academic family, Dr. Lorraine Pillus, Dr. Emily Petty, and all the members of the Pillus lab. Thank you for your mentorship, guidance, and encouragement throughout my undergraduate and graduate career. Thank you for always inspiring me and offering me the opportunity to fall in love with science and research.

To my biological family, my parents and my grandparents. Thank you for providing me the opportunity to live in the United States and pursue what I truly love. Your love, your support and your teaching have helped me immensely in times of difficulty and hardship.

To my American/Cuban family, Bryan Leon and his family. Thank you for taking care of me and for providing me with the warmth of a family while mine was on the opposite side of the earth. I spent a lot of time alone in the US but thanks to you I am seldomly lonely.

EPIGRAPH

围在城里的人想逃出去，城外的人想冲进去，
对婚姻也罢，职业也罢，人生的愿望大都如此

钱钟书，围城，1947

In a fortress besieged, those who are outside want to get in, and those who are inside want to get out. The same holds true for marriage, for career, and for most of our aspirations in life

Zhongshu Qian, *Fortress Besieged*, 1947

TABLE OF CONTENTS

LIST OF FIGURES

LIST OF TABLES

LIST OF ABBREVIATIONS, GENE NAMES, AND NOMENCLATURES

Cse4: A centromeric specific histone proteins

Cse4-S135: Serine residue 135 on the centromeric specific H3-like histone Ces4

Cse4-S135A: Cse4 with alanine on position 135 instead of serine, prevent phosphorylation of this residue

Cse4-S180: Serine residue 180 on the centromeric specific H3-like histone Ces4

Cse4-S180A: Cse4 with alanine on position 180 instead of serine, prevent phosphorylation of this residue

Cse4-S180DD: Cse4 with two aspartic acids on position 180 instead of serine, mimicking phosphorylation of this residue

D: Aspartic Acid

E: Glutamic Acid

Gcn5: A histone acetyltransferase protein

GCN5: Wild-type genes encoding Gcn5 protein

gcn5Δ: GCN5 knock out mutation

H2B-T91: Threonine residue 91 on histone H2B

H2B-T91A: Histone H2B with alanine on position 91 instead of threonine, prevents phosphorylation of this residue

H2B-T91E: Histone H2B with glutamic acid on position 91 instead of threonine, mimicking phosphorylation of this residue

H3-K14ac: Acetylation of lysine 14 on histone H3

H3-S10ph: Phosphorylation of serine 10 on histone H3

HAT: Histone acetyltransferase

HDAC: Histone deacetylase

Hog1: A yeast MAPK governing stress response to hyperosmolarity

Hsl1: A septin-binding kinases involved in morphogenesis checkpoint

Hsl7: A protein arginine methyltransferase, phosphorylated by Hsl1

HTB1: gene encoding WT histone H2B

htb1-T91A: gene encoding mutated histone H2B-T91A

K: Lysine

kinxΔ: kinase of interest knock out mutation

PP2A: Protein phosphatase 2A

$PP2A^{Rts1}$: A isoform of protein phosphatase 2A that contains the type-B regulatory subunit Rts1

Rts1: A Type-B regulatory protein of PP2A

RTS1: Wild-type gene encoding Rts1 protein

S: Serine

SAGA: A Gcn5 containing histone acetyltransferase complex

TAFs: TATA-Box binding protein associated factors

ACKNOWLEDGEMENTS

I would like to acknowledge Dr. Lorraine Pillus for her support and mentorship. Her insights and guidance are truly invaluable not only in the process of composing this thesis, but also in my future career development.

I would like to acknowledge Dr. Emily Petty. Without her teaching and her encouragement, I would not have the capacity or confidence to perform research and compose this thesis

I like to acknowledge the current members of Pillus Lab, Dr. Jennifer Chik, Stephen Klepin, Jessica Raygoza, and Brooke Michalik. Thank you for your support and help throughout my graduate studies.

Chapter 1, in part is currently being prepared for submission for publication of the material. Liu, Qihao; Petty, Emily; Pillus, Lorraine. The thesis author was the primary investigator and author of this material.

Chapter 2, in part is currently being prepared for submission for publication of the material. Liu, Qihao; Petty, Emily; Pillus, Lorraine. The thesis author was the primary investigator and author of this material.

Chapter 3, in part is currently being prepared for submission for publication of the material. Liu, Qihao; Petty, Emily; Pillus, Lorraine. The thesis author was the primary investigator and author of this material.

Chapter 4, in part is currently being prepared for submission for publication of the material. Liu, Qihao; Petty, Emily; Pillus, Lorraine. The thesis author was the primary investigator and author of this material.

ABSTRACT OF THE THESIS

Functional Tug of War between Hog1 and Gcn5, $PP2A^{Rts1}$ at the Spindle Assembly Check Point

by

Qihao Liu

Biology

University of California San Diego, 2022

Professor Lorraine Pillus, Chair

Covalent modifications of chromatin regulate genomic structure and accessibility in diverse biological processes such as transcriptional regulation, cell cycle progression, and the DNA damage response. Whereas many histone modifications have been characterized, understanding the interactions between these and their combinatorial effects remains an active area of investigation, including dissecting functional

interactions between enzymes mediating these modifications. In budding yeast, the histone acetyltransferase Gcn5 interacts with Rts1, the regulatory subunit of protein phosphatase 2A (PP2A), in part via the dynamic phosphorylation of conserved residues on histone H2B and the centromeric-specific histone H3 variant, Cse4. To further probe these dynamics, we sought to identify kinases which might contribute and found a role for a stress-activated protein kinase, Hog1. Deletion of *HOG1* (*hog1*Δ) rescues *gcn5*Δ sensitivity to the microtubule poison nocodazole and the lethality of the *gcn5*Δ *rts1*Δ double mutant. Dynamic phosphorylation of histone H2B-T91 also functions in the Hog1-Gcn5 interaction. Furthermore, Loss of *HOG1* decreases aneuploidy and apoptotic populations in *gcn5*Δ cells. Together, these results suggest that Hog1 functionally opposes Gcn5 and Rts1 in the context of the spindle assembly checkpoint and raise the possibility of further kinase involvement in *GCN5*'s functions.

Chapter 1: Introduction

Gcn5-mediated Histone Acetylation Alters Chromatin Structure:

Genetic materials in eukaryotic cells are neatly packaged into the complex named Chromatin. Chromatin is composed of DNA and the associated proteins. The basic repeating units of chromatin are nucleosomes, containing a histone octamer and a unit length of DNA wrapped around the core histones (Figure 1A). A histone octamer consists of two heterodimers of the canonical histones H2A, and H2B, and a tetramer of canonical histones H3, and H4. Histone proteins provide structural support to eukaryotic genetic materials. Furthermore, the replacement of canonical histones by the noncanonical variants allows the differentiation of chromatin: In budding yeast, *S. cerevisiae*, a centromere-specific H3-like histone variant, Cse4, differentiates the centromeric region from the rest of the chromatin (Meluh et al., 1998). Furthermore, Cse4 also mediates important cellular functions such as chromosome segregation and kinetochore functions (Meluh et al., 1998).

Beyond substitution of canonical histones, chromatin also undergoes dynamic modifications, providing an additional layer of complexity to chromatin structure and functions. Enzymes known as chromatin modifiers can attach or remove small covalent groups onto or from specific residues on the globular domain and N-terminal tails of histone proteins. Histone modifications, such as acetylation, phosphorylation, methylation, and ubiquitination, regulate chromatin structure, alter the interaction between histones and DNA, and recruit nonhistone proteins; the dynamic modifications of core histones play a crucial role in various cellular processes such as transcriptional regulation, DNA damage repair, and DNA replication (Koumanidis, 2007). Among the

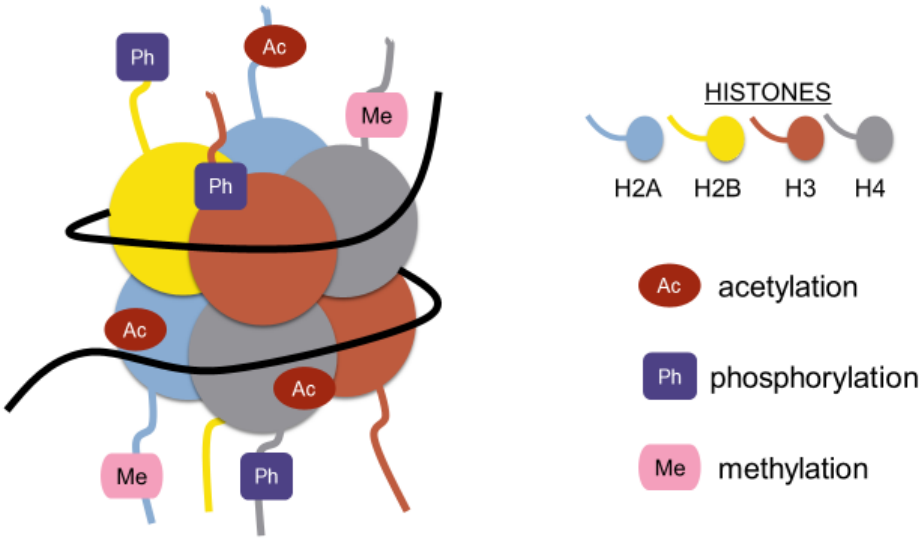

Figure 1A **Nucleosome is the basic repeating unit of chromatin.** Chromatin is composed of DNA and associated proteins. The basic repeating unit of chromatin is the nucleosome, composed of two heterodimers of the core histones H2A, and H2B, and a tetramer of core histones H3, and H4. Histones have unstructured N-terminal tails that are subjected to covalent modifications such as phosphorylation, acetylation, and methylation.

histone modifications, lysine (K) acetylation, the addition of an acetyl group onto a histone lysine residue, can disrupt the interaction between the positively charged lysine residue and the negatively charged DNA, making the DNA more accessible to cellular machineries. Thus, histone acetylation has been found to be closely correlated with open-chromatin and transcription regulation (Barnes et al., 2019). Loss of histone-modifying enzymes mediating dynamic histone acetylation, such as histone acetyltransferases (HAT) and histone deacetylase (HDAC), produces a considerable impact on multiple cellular processes.

Furthermore, histone modifications do not function in isolation. Crosstalk between histone modifications adds an extra level of control to chromatin modifications: one modification on a histone residue can affect the occurrence of other modifications in the same or neighboring histones (Bannister & Kouzarides, 2011). A previous study showed that phosphorylation of histone H3 serine 10 (H3-S10ph) promotes acetylation of histone H3 lysine 14 (H3-K14ac), a histone marker associated with upregulated gene transcriptions (Lo et al., 2000). Another study also suggests methylation of histone H3 residues is closely linked to ubiquitination and methylation of multiple H2B residues (Wyce et al., 2007). These results depict a complex network of interaction between chromatin modification and chromatin modifiers. Thus, further investigation of the crosstalk between chromatin modification and associated enzymes facilitates a better understanding of chromatin biology.

Gcn5 is a well-conserved histone/lysine acetyltransferase (H/KAT) in eukaryotes involved in transcriptional regulation (Imoberdorf et al., 2006), transcriptional elongation (Xue-Franzén et al., 2013), DNA replication (Espinosa et al., 2010), nucleosome

assembly (Burgess & Zhang, 2010), and DNA damage repair (Tamburini & Tyler, 2005). In budding yeast, *Saccharomyces cerevisiae*, the histone acetyltransferase (HAT) Gcn5 functions in three distinct histone acetyltransferase complexes: ADA, SAGA, and SLIK/SALSA (Eberharter et al., 1999; Grant et al., 1997; Sterner et al., 2002) (Figure 1B). The multi-subunit and multi-functional SAGA complex contain the HAT module (Figure 1B), including Gcn5, Sgf29, Ada2 and Ada3, the TATA-box binding protein (TBP) associated factors (TAFs) module (Taf5, Taf6, Taf9, Taf10, Taf12), DUB module (Ubp8, Sus1, Sgf11, Sgf73), and transcriptional regulatory module (Spt3, Spt7, Spt8, Spt20, Ada1, Tra1) (Baker & Grant, 2007; Liu et al., 2019). The Gcn5-containing SAGA complex mediates transcription regulation of genes that respond to environmental stress whereas the well-known TFIID mediates transcription regulation of "housekeeping" genes (Huisinga & Pugh, 2004). Similar in structure to SAGA, the Gcn5-containing SLIK/SALSA complex is distinguished from the SAGA complex by the absence of Spt8 and the presence of Rtg2 (Baker & Grant, 2007; Sterner et al., 2002). The SLIK/SALSA complex function in the retrograde signaling pathway, communicating mitochondria dysfunction to the nucleus (Baker & Grant, 2007; Jazwinski, 2013). Compared to SAGA and SLIK/SALSA, the ADA complex is much smaller, containing only the HAT module of SAGA (Gcn5, Sgf29, Ada2, Ada3) along with two structural subunits Ahc1 and Ahc2 (Grant et al., 1997). The ADA complex is involved in histone crotonylation which was dynamically regulated in the yeast metabolic cycle (Gowans et al., 2019; Kollenstart et al., 2019). In *S. cerevisiae*, deletion of genes encoding key subunits of SAGA induces temperature sensitivity and DNA damage sensitivity (Petty et al., 2016). Gcn5 is also identified as an important factor in the transcriptional regulation

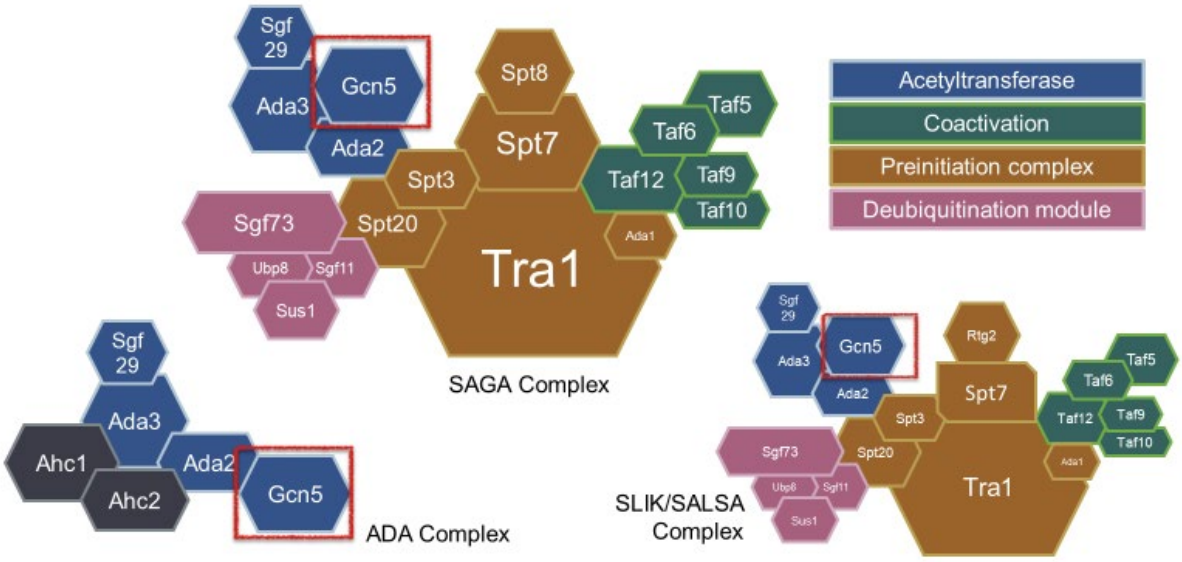

Figure 1B **Gcn5 is the catalytic subunit of the multi-functional SAGA and SLIK/SALSA complexes and the smaller ADA complex.** The multi-subunit, multifunctional SAGA Complex contains a HAT module (Gcn5, Sgf29, Ada2, Ada3) (Blue), a TATA-box binding protein (TBP) associated factors (TAFs) module (Taf5, Taf6, Taf9, Taf10, Taf12) (Orange), DUB module (Ubp8, Sus1, Sgf11, Sgf73) (Purple), and transcriptional regulatory module (Spt3, Spt7, Spt8, Spt20, Ada1, Tra1) (Green). The SLIK/SALSA complex contains similar modules to Gcn5, except for Rtg2 and a truncated version of Spt7. Smaller Gcn5-containing ADA complex has unique structural subunit Ahc1 and Ahc2 (grey) in addition to the HAT module components (Modified from Lee et al, 2011).

of oncogenic genes (Nagy & Tora, 2007). Upregulation of oncogenic gene, resulting from changes in Gcn5 HAT activity, is observed in various human cancers such as colon cancer (Yin et al., 2015), hepatocellular carcinoma (Majaz et al., 2016), and lung cancers (Mustachio et al., 2019). Further study and elucidation of the function of Gcn5 will provide insight into the transcriptional and cellular events that contribute to cancer development.

While the importance of Gcn5-mediated histone acetylation is well-documented, the interdependency between other forms of histone modification and Gcn5-mediated histone acetylation remains an area of active investigation. Understanding the functional association between *GCN5* and other genes is the first step toward elucidation of the complex interactional network in which Gcn5 and its associated histone acetylation are embedded. Genetic screen, a method used to identify desired phenotypes within a mutant population, provides a powerful tool to identify genes that functionally interact with *GCN5*. Since Gcn5 plays a significant role in various cellular events, Loss of *GCN5* is not tolerated in many eukaryotic models such as *D. melanogaster* (Carré et al., 2005) and *M. musculus* (Bu et al., 2007). in *S. cerevisiae*, knockout of Gcn5 is tolerated but causes a variety of phenotypes, including temperature sensitivity, DNA damage sensitivity, poor growth on non-fermentable carbon sources, and chromosome segregation defects (Cherry et al., 2012; Petty et al., 2016). Previously, by altering gene dosage in the *gcn5Δ* background and selecting mutants based on alleviation of *gcn5Δ* phenotypes, the Pillus lab revealed genetic interaction between *GCN5* and *RTS1*, a gene encoding the regulatory subunit of protein phosphatase 2A (PP2A) (Petty et al., 2016).

RTS1 is Identified as a Dosage Suppressor of *gcn5Δ* phenotypes:

RTS1 is identified as a dosage suppressor of a variety of *gcn5Δ* phenotypes: Overexpression of *RTS1* in *gcn5Δ* mutant rescues temperature sensitivity, DNA damage sensitivity, poor growth on non-fermentable carbon sources, and chromosome segregation defects of *gcn5Δ* mutant (Petty et al., 2016). In budding yeast, *RTS1* encodes one of the two highly conserved type-B regulatory subunits of protein phosphatase 2A (PP2A) (Healy et al., 1991; Shu et al., 1997). PP2A is a heterotrimeric serine/threonine phosphatase complex containing a type-A regulatory subunit (van Zyl et al., 1992), a catalytic subunit, and either type-B regulatory subunit (Sneddon et al., 1990) (Figure 1C). In mammalian cells, PP2A attenuates cancer progression by counterbalancing phosphorylation of oncoproteins via its phosphatase activities (Perrotti & Neviani, 2013)

In *S. cerevisiae*, Rts1-containing PP2A ($PP2A^{Rts1}$) is recruited to the centromeric region to promote spindle assembly checkpoint and cell cycle progression (Jiang, 2006; Nerusheva et al., 2014). Beyond its involvement in cell cycle progression, Rts1 also controls glucose-induced activation of PP2A (Castermans et al., 2012), suggesting a role for $PP2A^{Rts1}$ in nutrient response. Though the cellular function of $PP2A^{Rts1}$ is well-understood, whether $PP2A^{Rts1}$ is involved in mediating chromatin modifications remains unclear. Petty et al. reported that deletion of genes encoding either the type-A regulatory subunit, the catalytic subunit, or *RTS1* causes lethality in *gcn5Δ* background (Petty et al., 2016), indicating that a functionally intact $PP2A^{Rts1}$ is crucial to the *gcn5Δ* mutant. Furthermore, *RTS1* overexpression also rescues temperature sensitivity and DNA damage sensitivity observed in various SAGA mutants (Cherry et al., 2012; Petty

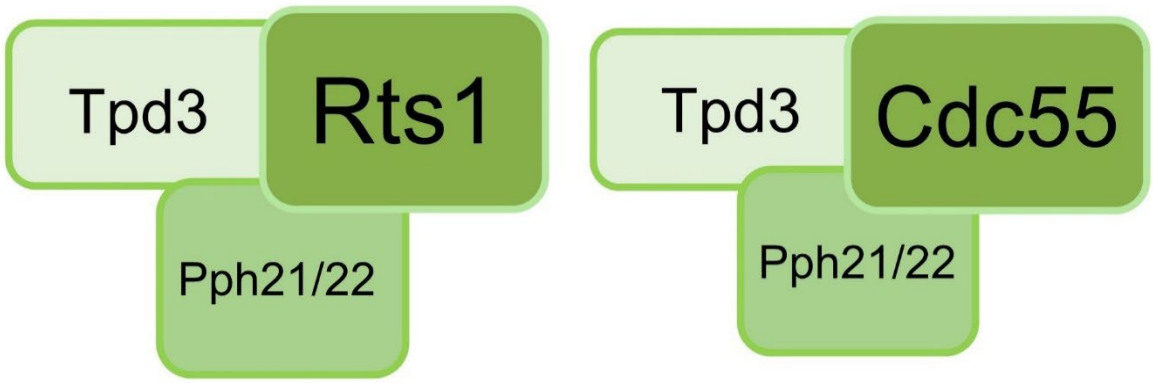

Figure 1C ***RTS1* encodes one of the two regulatory subunits of PP2A.** PP2A is a heterotrimeric serine/threonine phosphatase complex containing type-A regulatory subunit Tpd3 (purple), type-B regulatory subunit Rts1/Cdc55 (Green), and catalytic subunit Pph21/Pph22 (pink). (Modified from Jiang et al, 2006)

et al., 2016). These results suggest that Rts1 and Gcn5 interact as part of the $PP2A^{Rts1}$ and SAGA Complexes. Since SAGA Complex acetylates histone H3 (Baker & Grant, 2007), modification of specific histone residues maybe involved in the dosage-dependent Rts1-Gcn5 interaction. *RTS1* overexpression restores global histone H3 acetylation level in *gcn5Δ* mutants (Petty et al., 2016), further implying that increased dephosphorylation caused by over-expression of Rts1 might promote H3 acetylation. Therefore, crosstalk between $PP2A^{Rts1}$ mediated histone dephosphorylation and Gcn5 mediated histone acetylation is likely involved in the dosage-dependent rescue of the *gcn5Δ* phenotypes by *RTS1*.

Threonine 91 residue on histone H2B (H2B-T91) is identified as an important player in the Rts1-Gcn5 interaction (Petty et al., 2016). Surprisingly, the *htb1-T91A* mutation, which abolishes H2B-T91 phosphorylation by replacing the threonine residue with an alanine, hinders the rescue of *gcn5Δ* phenotypes by *RTS1* overexpression instead of alleviating *gcn5Δ* phenotypes in a similar fashion as *RTS1* overexpression (Petty et al., 2016). Though the result failed to show that dephosphorylation of histone residue is crucial to *gcn5Δ* mutants, it indeed confirmed that specific histone residue is involved in Rts1-Gcn5 interaction. Since the phosphodeficient *htb1-T91A* mutation hinders the rescue of *gcn5Δ* phenotypes by *RTS1* overexpression, a phosphomimic mutation of H2B-T91 (*htb1-T91E*) in the *gcn5Δ* background might cause opposite effect as the *htb1-T91A* mutation. However, the phosphomimic *htb1-T91E* mutation results in lethality (Petty et al., 2016). Both the phosphodeficient and phosphomimic mutation of H2B-T91 causes defects in *gcn5Δ* background, suggesting that the lack of ability to dynamically phosphorylate and dephosphorylate the histone residue H2B-T91 is

detrimental to *gcn5Δ* cells. These data suggest that the dynamic phosphorylation of H2B-T91 is crucial in the Rts1-Gcn5 interaction.

Dynamic phosphorylation, the attachment and removal of a phosphate group, allows tunable responses via phosphatase and kinase activity (Ardito et al., 2017). Changes in phosphorylation states have a profound impact on the localization, activity, and conformation of the proteins (Mok et al., 2011). Dynamic histone phosphorylation has a significant role in different cellular processes such as DNA damage response and transcription regulation, but it also plays a role in chromatin compaction during mitosis, meiosis, and apoptosis (Rossetto et al., 2012). Since the dynamic phosphorylation of histone residues likely underlies the functional interaction between *RTS1* and *GCN5*, we hypothesized that a kinase may also function as part of the Rts1-Gcn5 interaction network. Such a kinase and $PP2A^{Rts1}$ work together to mediate dynamic phosphorylation on histone residues that are likely important for Gcn5 functions (Figure 1D). Since overexpression of Rts1 potentially biases the chromatin phosphorylation balance towards the dephosphorylated states, loss of the kinase that shares the same substrate with $PP2A^{Rts1}$ should achieve the same effect, suppressing similar phenotypes in the *gcn5Δ* background as *RTS1* overexpression does. To test for this hypothesis, a genetic screen was performed.

A Missing Kinase involved in the *RTS1-GCN5* Interaction:

Investigation of the kinase that is involved in the Rts1-Gcn5 interaction reported by Petty et al. requires us to identify the kinases mutant via a genetic screen, confirm that the identified kinase is involved in Rts1-Gcn5 interaction by the rescue of *gcn5Δ rts1Δ* synthetic lethality, identify histone residues involved in the Kinase-Gcn5

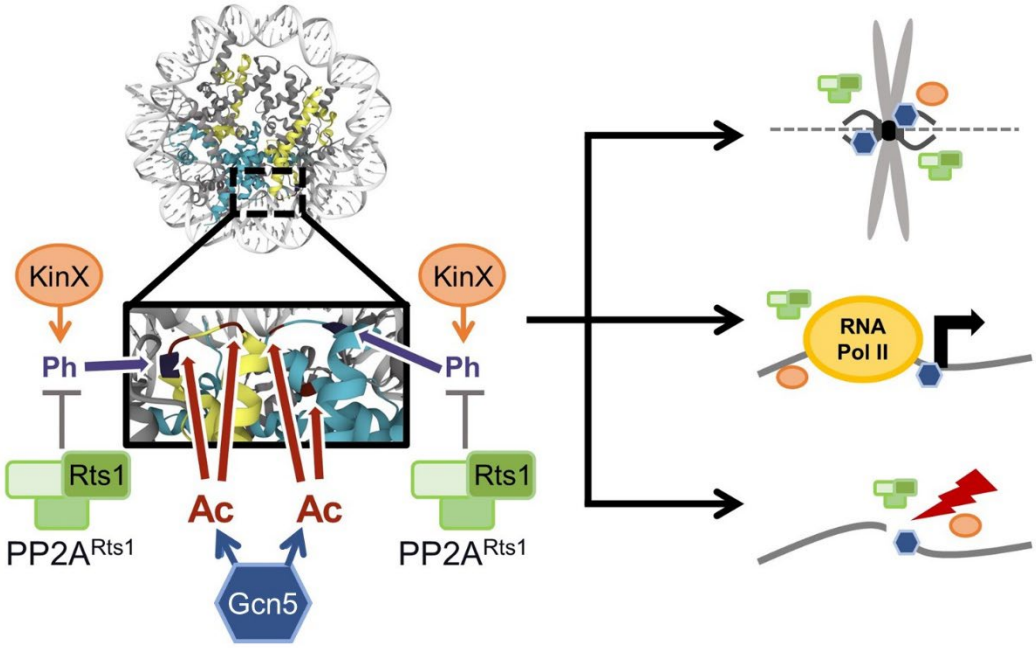

Figure 1D **A Kinases might be Involved in the *RTS1-GCN5* Interaction.** Overexpression of the gene encoding a regulatory subunit of protein phosphatase 2A (PP2A, green), *RTS1*, rescues a variety of phenotypes caused by deletion of *GCN5* (dark blue) the gene encoding the histone acetyltransferase module's (HAT) catalytic subunit of the SAGA complex (Petty et al., 2016). Genetic screens demonstrated that dynamic phosphorylation of specific H2B histone residues is important for the Rts1-Gcn5 interaction. Thus, there may be a kinase or kinases (denoted as KinX) functioning in the *RTS1-GCN5* interaction nexus. We hypothesize that deletion of such a kinase would rescue the same set of *gcn5*Δ phenotypes suppressed by *RTS1* overexpression, whereas overexpression of the gene encoding the kinase may result in lethality in *gcn5*Δ cells.

interaction, and dissect the underlying mechanism of the functional interaction.

By examining the changes of a specific phenotype resulting from a combination of mutations, the genetic screen elucidates the functional interdependencies between genes underlying certain phenotypes. Since the previous result showed that *RTS1* overexpression rescues *gcn5Δ* phenotypes. Deletion of a kinase gene that is involved in the *RTS1-GCN5* interaction should also rescues the same set of *gcn5Δ* phenotypes. To screen for kinase mutant of interest (denoted as *kinxΔ*), *gcn5Δ kinxΔ* double mutants are constructed and tested with growth assay under various experimental conditions (Boutros & Ahringer, 2008) (Figure 1E). An improvement in growth in the double mutant compared to the *gcn5Δ* single mutant under specific experimental conditions indicate suppression of *gcn5Δ* phenotypes. The initial genetic screen indicates that loss of the genes encoding either the nuclear kinase Hog1 or Kss1 rescues *gcn5Δ* chromosome segregation defect and genotoxic stress sensitivity respectively (Chapter 2). Therefore, genetic interactions between *KSS1*/*HOG1* and *GCN5* were identified. Synthetic lethality occurs when the combination of two mutations produces an extremely serve phenotype that results in cell death. *hog1Δ* and *kss1Δ* were reported as suppressors of *gcn5Δ rts1Δ* synthetic lethality, confirming that *KSS1* and *HOG1* are involved in the *RTS1-GCN5* interaction

Furthermore, the catalytic activity of Hog1 was found to provide an underlying mechanism for the Hog1-Gcn5 interaction (Chapter 3). Mutations on the histone H2B-T91 residue abolish the suppression of *gcn5Δ* phenotypes by *hog1Δ* (Chapter 3), indicating that the same phosphorylatable histone residue underlies both *RTS1-GCN5* interaction and *HOG1-GCN5* interaction.

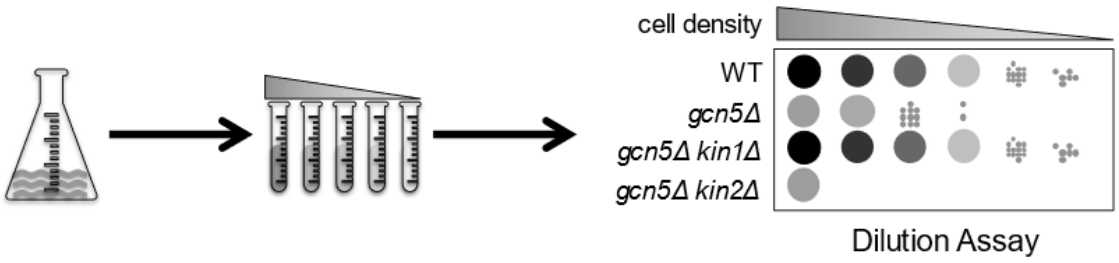

Figure 1E **Semiquantitative growth assay allows for the comparison of the relative growth of different strains under specific conditions.** Through semiquantitative growth assay, we analyzed the relative growth of Wild Type, *gcn5Δ*, kinase deletion (denoted as *kinxΔ*), and *kinxΔ gcn5Δ* strains under a variety of experimental conditions. Semiquantitative growth assay allowed identification of rescue of *gcn5Δ* phenotypes by *kinxΔ* when the relative growth of *kinxΔ gcn5Δ* was restored to the wild-type level.

In chapter 4, cell cycle studies were conducted to further dissect the interaction between *GCN5* and *HOG1*. *hog1Δ* failed to rescue *gcn5Δ* defective cell cycle under normal conditions but reduces the amount of aneuploidy and apoptotic population in *gcn5Δ* mutant during nocodazole treatment, suggesting that Hog1 and Rts1 might not necessarily function on a shared target in the context of chromosome segregation: Whereas increased dosage of *RTS1* promotes spindle assembly checkpoint to counterbalance the effect of nocodazole, *hog1Δ* may achieve the same effect via suppression of mitotic exit.

Chapter 1, in part is currently being prepared for submission for publication of the material. Liu, Qihao; Petty, Emily; Pillus, Lorraine. The thesis author was the primary investigator and author of this material.

Chapter 2: A genetic screen identifies kinases with potential interactions with *GCN5*

Introduction:

The ability to respond to and adapts changes in the extracellular environment is crucial for the survival of organisms. In their natural environment, yeast cells are exposed to a variety of stress, such as heat shock, DNA damage, nutrient limitation, and osmotic stress. Rapid molecular responses ensure these simple eukaryotes can survive and proliferate. A common underlying mechanism behind various stress responses in budding yeast is the change in gene expression, and histone modification helps mediate the transcriptional modulations during stress response; histones are found to be dynamically modified when budding yeasts are exposed to osmotic stress (Magraner-Pardo et al., 2014), DNA damage (Kim et al., 2019), and heat shock stress (Erkina & Erkine, 2006).

The expression of many stress-inducible genes depends on the Gcn5-containing SAGA complexes (Huisinga & Pugh, 2004). Yeast cells lacking Gcn5 show decreased activation of genes crucial for osmotic stress and oxidative stress responses (Lee et al., 1999; Rep et al., 2001). Considering that histone acetylation contributes to the increased accessibility of chromatin to cellular machineries, as well as to the transcriptional upregulation of stress response genes, Gcn5-dependent acetylation of chromatin is important in the appropriate response to a variety of stress such as heat, oxidation, nitrogen starvation, and DNA damage (Huisinga and Pugh, 2004). Gcn5-dependent H3 acetylation is linked to transcriptional upregulation of genes encoding the heat-shock protein (Hsp) which plays an important role in ensuring correct protein

folding during stress exposure (Han et al., 2008). Furthermore, Gcn5-dependent H3K36 acetylation, a histone modification abolished in *gcn5Δ*, promotes homology-directed repair in response to double-strand break (Pai et al., 2014), indicating Gcn5's involvement in DNA damage repair pathways. Together, these results suggest that Gcn5-mediated histone acetylation is an integral part of many stress responses crucial for the survival of the cell. Therefore, loss of Gcn5 causes sensitivities to many forms of stress.

When the combination of two mutations results in the restoration of a mutant phenotype to wildtype level, the suppression indicates a functional association between two genes. *RTS1* overexpression rescues *gcn5Δ* sensitivity to various stresses (Petty et al., 2016), indicating a functional interaction between *RTS1* and *GCN5*. Since dynamic phosphorylation on H2B was suspected to provide an underlying mechanism for *RTS1-GCN5* interaction (Petty et al., 2016), a kinase was hypothesized to be involved in the *RTS1-GCN5* interaction. To identify the kinase that functionally interacts with Rts1 and Gcn5, a genetic screen was performed to select for suppression of known *gcn5Δ* phenotypes by kinase deletion.

In this chapter, we have identified two nuclear kinase genes, *HOG1* and *KSS1*, to be involved in the *RTS1-GCN5* interaction. Hog1 and Kss1 belong to a family of protein kinase known as mitogen activated protein kinases (MAPKs). MAPKs are conserved serine/threonine kinases in eukaryotes involved in signal transduction pathways, converting extracellular signals to intracellular responses. In yeast, Hog1 governs the cellular responses to changes in extracellular osmolarity and salt concentration (Brewster et al., 2014), and Kss1 mediates filamentous growth in response to nutrient

limitation (Morillon et al., 2000). When extracellular stresses are sensed by membrane sensors, mitogen-activated protein kinase kinase kinase (MAPKKK) activates the mitogen-activated protein kinase kinase (MAPKK), which in turn phosphorylates the target MAPK, allowing the MAPK to perform its stress-response functions (Maayan et al., 2012; Maeda et al., 1995; Posas et al., 1996). Dysregulations of the mammalian homolog of Hog1 and Kss1, P38 and Erk1/2, are both found to be associated with multiple forms of cancer, including liver cancer (Guégan et al., 2012; Wang et al., 2012), lung cancer (Crosbie et al., 2016; Koul et al., 2013), and colon cancer (Randhawa et al., 2013; Yang et al., 2011), suggesting the MAPKs are prominent therapeutic targets for many forms of cancer. By investigating the interaction between genes encoding MAPKs, *GCN5*, and *RTS1*, we hope to expand our current knowledge of the roles played by MAPK in the context of chromatin biology and stress response.

Results:

Saccharomyces Genome Database Allows Identification of Nuclear Kinase:

To identify kinases that might function in the *GCN5-RTS1* interaction, we first surveyed the 127 genes encoding protein kinases (Rubenstein & Schmidt, 2007) in budding yeast via the Saccharomyces Genome Database (Cherry et al., 2012). Considering that the *GCN5-RTS1* nexus involves specific histone residues (Petty et al., 2016), we hypothesized that a kinase participating in the nexus was likely to include nuclear functions. Of the yeast kinases, 38 genes encoding nuclear kinases were identified. Analysis of curated information of kinases in DNA damage repair, cell cycle progression, stress/nutrient responses, and interaction with Gcn5 and Rts1 identified 18 candidate genes meeting these criteria (denoted as *KINX*) (Figure 2A, Table 2.1):

CDC28, CHK1, CKA1, CKA2, CLA4, CTK1, DUN1, HOG1, IPL1, KSS1, PHO85, RAD53, SCH9, SLT2, SNF1, STE20, SWE1, and *TEL1*(Cherry et al., 2012).

5-Fluoroorotic acid (5-FOA) counter selection allows identification of viable *gcn5*Δ double mutant:

Synthetic lethality is induced when two or multiple mutations are combined and produce a nonviable phenotype. The viability of *gcn5*Δ kinase knock-out double mutant (*gcn5*Δ *kinx*Δ) must be ensured prior to phenotypic analysis (Figure 2A). In cells expressing *URA3* genes, the chemical 5-FOA is converted into a toxic compound 5-fluorouracil, preventing the cells with the *URA3* gene from growing on 5-FOA containing media (Boeke et al., 1987). *gcn5Δ kinxΔ* double mutants were constructed bearing a *URA3*-tagged *GCN5* plasmid. Semiquantitative growth assay on solid media containing 5-FOA was performed for the identification of viable *gcn5Δ kinxΔ*: Since *GCN5-URA3* plasmid is essential for *gcn5Δ kinxΔ* with synthetic lethality, and 5-FOA is converted to a toxic compound by the protein product of *URA3*, only *gcn5Δ kinxΔ* that does not require a copy of *GCN5* grow on the 5-FOA solid media.

Among genes encoding cell cycle kinases, *swe1*Δ *gcn5*Δ, *pho85*Δ *gcn5*Δ and *chk1*Δ *gcn5*Δ showed growth on the 5-FOA medium (Figure 2B), indicating that they were viable double mutants. Since *CDC28* and *IPL1* are essential genes in budding yeast, and deletion of which causes lethality, *cdc28*Δ *gcn5*Δ and *ipl*Δ *gcn5*Δ were not included in the synthetic lethality screen. As for genes encoding nutrient and stress response kinases, *snf1*Δ *gcn5*Δ*, sch9*Δ *gcn5*Δ*, kss1*Δ *gcn5*Δ*,* and *hog1*Δ *gcn5*Δ showed growth on the 5-FOA plates, indicating that most of the gcn5Δ nutrient/stress response kinase deletion double mutants are viable (Figure 2C). The viability of the *ste20*Δ *gcn5*Δ

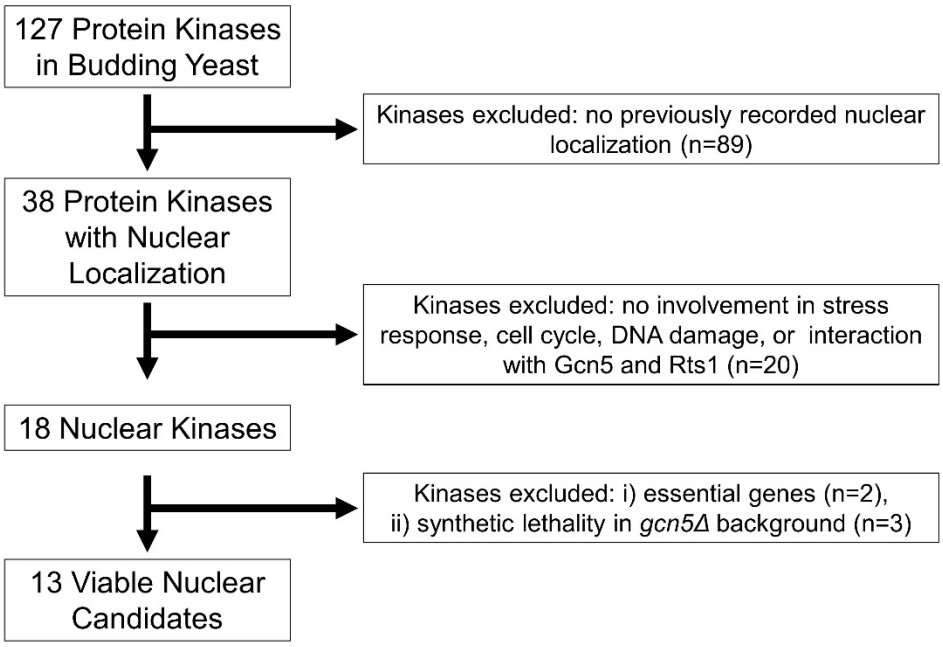

Figure 2A **13 kinases of interest were selected based on nuclear localization, cellular functions, interaction with *GCN5* and/or *RTS1*, and viability of the null mutation in the *gcn5Δ* background.** The127 kinases encoded in the yeast proteome were first screened for nuclear localization recorded in the Saccharomyces Genome Database. 38 kinases with some evidence of nuclear localization were identified. Because *RTS1* overexpression specifically suppresses *gcn5*Δ various sensitivities the kinase candidates were categorized based on their involvement in nutrient and stress response, cell cycle progression, DNA damage, and interactions with *GCN5* and *RTS1*. 17 kinases meet these criteria. Since the deletion of the nuclear kinase was hypothesized to rescue *gcn5*Δ phenotypes, the *gcn5*Δ *kinx*Δ double mutant must be viable. Therefore, two essential nuclear kinases and three kinases, the deletion of which causes serve sickness or lethality in *gcn5*Δ background, were excluded from the list of candidates, yielding 13 nuclear kinases for further genetic analysis.

Table 2.1 **18 genes encoding nuclear kinases were selected based on recorded physical and genetic interaction with Gcn5 and Rts1.**

Cell Cycle	*PHO85, SWE1, CHK1, CDC28,IPL1,CLA4*
Nutrient/Stress Response	*SNF1, KSS1, SCH9, SLT2, STE20, HOG1*
Transcription/ DNA Damage	*CTK1, DUN1, CKA1, CKA2, TEL1, RAD53*

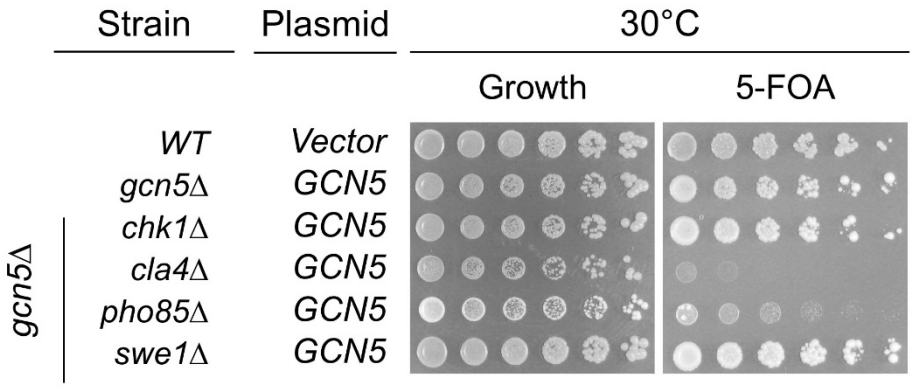

Figure 2B **Loss of *SWE1* or *CHK1* is not lethal in *gcn5*Δ mutant.** WT (LPY 5), *gcn5*Δ (LPY 13319), *gcn5*Δ *pho85*Δ (LPY 18491), *gcn5*Δ *swe1*Δ (LPY 23013), *gcn5*Δ *chk1*Δ (LPY 20298), and *gcn5*Δ *cla4*Δ (LPY 23002) were transformed with pLP 1640 (*CEN-URA3-GCN5*). Cells were plated onto URA- (growth) as well as 5-FOA plate and incubated at 30°C for three days.

double mutant was confirmed by a previous study (data not shown). Among genes encoding transcription and DNA-damage related kinases, *ctk1*Δ *gcn5*Δ*, dun1*Δ *gcn5*Δ*, cka1*Δ *gcn5*Δ*, cka2*Δ *gcn5*Δ*,* and *tel1*Δ *gcn5*Δ were identified as viable double mutants based on growth on 5-FOA plate (Figure 2D). Out of the 18 genes encoding nuclear kinases, we identified 2 essential genes, 3 synthetic lethality interactions and 13 genes that can be knocked out in the *gcn5*Δ background for further phenotypic analysis via semi-quantitative assay.

Deletion of nuclear kinases alleviates a variety of *gcn5*Δ phenotypes

Rescue of *gcn5*Δ phenotypes by deletion of genes encoding nuclear kinase implies potential interaction between the nuclear kinase and Gcn5. Via genetic screen under elevated growth temperature, DNA Damage, and chromosome segregation stress, we analyzed if deletion of kinase genes alleviates previously reported *gcn5*Δ phenotypes (Petty et al., 2016). *kinx*Δ *gcn5*Δ double mutants were plated onto media containing the microtubule poison nocodazole (NOC), DNA damage agent hydroxyurea (HU) and methyl methane sulfonate (MMS) or exposed to elevated growth temperature at 37 °C. *chk1*Δ*, hog1*Δ*,* and *kss1*Δ were identified as mutations that rescue *gcn5*Δ sensitivity to high growth temperature (Figure 2E), cell cycle progression defect (Figure 2.F), and DNA damage (Figure 2G) respectively. Interestingly, *kss1*Δ rescue of *gcn5*Δ sensitivity to DNA damage was observed in the *MATα* background, but not in the *MATa* background; *gcn5*Δ and *MATa kss1*Δ *gcn5*Δ showed strong growth defect on media containing HU and MMS whereas *MATα kss1*Δ *gcn5*Δ showed growth comparable to the wildtype on genotoxic agent-containing media (Figure 2G). Compared to the previous study, which identified that *RTS1* overexpression rescues a variety of

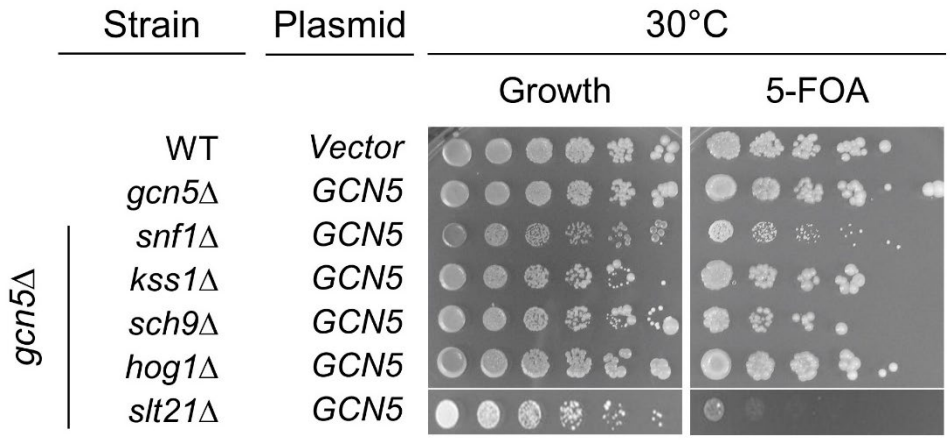

Figure 2C **Loss of *SNF1*, *KSS1*, *SCH9*, *HOG1*, or *SLT2* is not lethal in *gcn5*Δ mutant.** WT (LPY 5), *gcn5*Δ (LPY 13319), *gcn5*Δ *snf1*Δ (LPY 13440), *gcn5*Δ *kss1*Δ (LPY 18171), *gcn5*Δ *sch9*Δ (LPY 17138), and *gcn5*Δ hog*1*Δ (LPY 21366) were transformed with pLP 1640 (*CEN-URA3-GCN5*). Cells were plated onto URA- (growth) as well as 5-FOA plate and incubated at 30°C for three days.

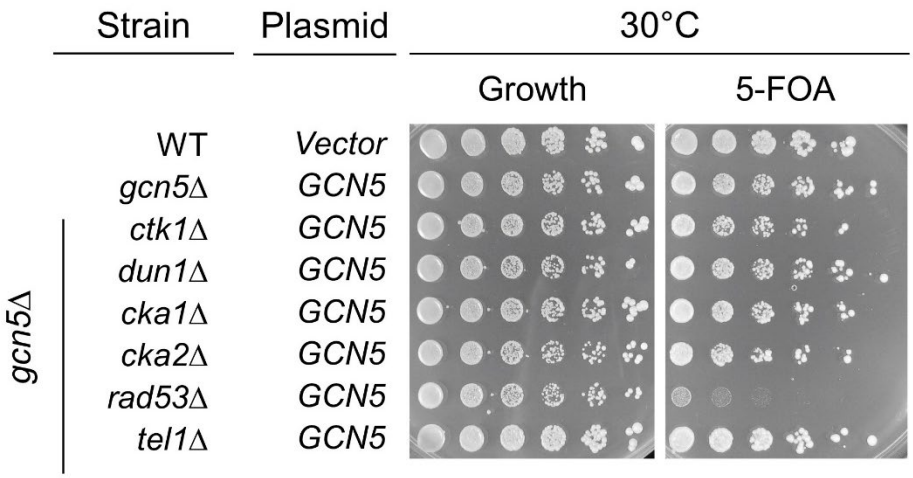

Figure 2D **Loss of *CTK1*, *DUN1*, *CKA1*, *CKA2*, or *TEL1* is not lethal in *gcn5*Δ mutant.** *WT* (LPY 5), *gcn5*Δ (LPY 13319), *gcn5*Δ *ctk1*Δ (LPY 20366), *gcn5*Δ *dun1*Δ (LPY 20370), *gcn5*Δ *cka1*Δ (LPY 21669), *gcn5*Δ *cka2*Δ (LPY 21373), *gcn5*Δ *rad53*Δ (LPY 21388), and *gcn5*Δ *tel1*Δ (LPY 20132) were transformed with pLP 1640 (*CEN-URA3-GCN5*). Cells were plated onto URA- (growth) as well as 5-FOA plate and incubated at 30°C for three days.

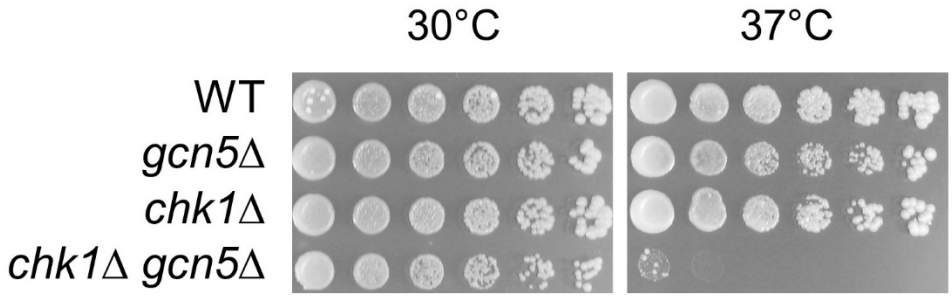

Figure 2E ***chk1*Δ Suppresses *gcn5*Δ temperature sensitivity.** Five-fold dilution of WT (LPY 5), *gcn5*Δ (LPY 13319), *chk1*Δ (LPY 20086), and *chk1*Δ *gcn5*Δ (LPY 20298) were plated onto YPAD plates placed at varying temperature (30°C, 37°C). Cells were incubated for three days. *chk1*Δ *gcn5*Δ shows suppression of *gcn5*Δ sensitivity to high temperature.

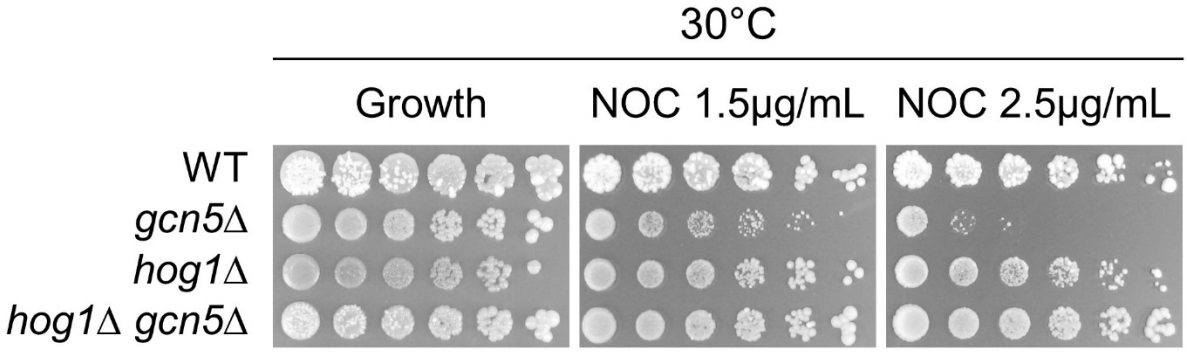

Figure 2F ***hog1*Δ rescues *gcn5*Δ nocodazole sensitivity.** Five-fold dilution of *wild type* (LPY 5), *gcn5*Δ (LPY 13319), *hog1*Δ (LPY 21374), and *hog1*Δ *gcn5*Δ (LPY 21366) were plated onto YPAD (growth) and nocodazole (NOC) plates with varying concentration. Cells were incubated at 30°C for three days.

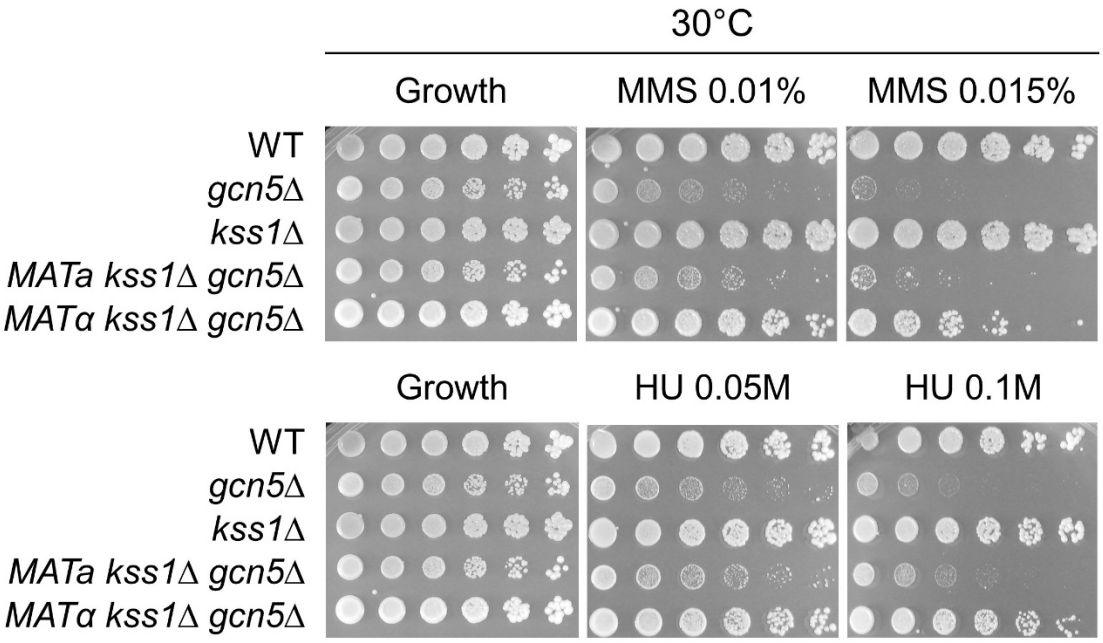

Figure 2G ***kss1*Δ rescues *gcn5*Δ DNA damage sensitivity.** Five-fold dilution of *MAT*a wild type (LPY 5), *MATa gcn5*Δ (LPY 13319), *MAT a kss1*Δ (LPY 1873), and *kss1*Δ *gcn5*Δ (*MATa* : LPY 18171; *MAT α*: LPY 18172) were plated onto synthetic complete (growth), hydroxyurea (HU) and methane sulfonate sensitivity (MMS) plates with varying concentration.

*gcn5*Δ phenotypes (Petty et al., 2016), we have found that deletion of genes encoding nuclear kinase only rescues a certain subset of the *gcn5*Δ phenotypes.

Beyond sensitivity to elevated temperature, microtubule poison, and genotoxic stress, we also found that *gcn5*Δ is sensitive to calcofluor white (CFW), a chemical compound that induces cell wall stress. Two deletions of genes encoding nuclear kinases rescue *gcn5*Δ sensitivity to CFW. *chk1*Δ partially rescues *gcn5*Δ sensitivity to CFW (Figure 2H). Interestingly, *hog1*Δ *gcn5*Δ showed growth comparable to WT on the CFW medium whereas both *hog1*Δ and *gcn5*Δ single mutant had difficulties growing on the medium containing CFW (Figure 2I). In conclusion, we observed that deletion of *HOG1* or *CHK1* in the *gcn5*Δ background suppresses *gcn5*Δ sensitivity to CFW. Together, these observations indicate that loss of nuclear kinase forms distinct patterns of suppression in *gcn5*Δ mutant. (Figure 2J).

Deletion of MAPK-encoding genes rescues ***gcn5*Δ *rts1*Δ** synthetic lethality.

Concurrent loss of Gcn5 and Rts1 induces synthetic lethality (Petty et al., 2016). Since we identified both *RTS1* overexpression and *hog1Δ, kss1Δ* as suppressors of *gcn5Δ* nocodazole and DNA damage sensitivity, we hypothesized that loss of Hog1 or Kss1 might rescue the *rts1Δ gcn5Δ* synthetic lethality. Therefore, a synthetic lethality screen is used to determine if loss of Kss1 or Hog1 can suppress *gcn5*Δ *rts1*Δ synthetic lethality. *kinx*Δ *gcn5*Δ *rts1*Δ triple mutants were constructed bearing a copy of the *URA3-GCN5* plasmid. Growth on 5-FOA medium indicates successful rescue of *gcn5*Δ *rts1*Δ synthetic lethality by the loss of kinase. Deletion of both *HOG1* and *KSS1* restores growth in *gcn5*Δ *rts1*Δ on 5-FOA medium, indicating that the gcn*5*Δ *rts1*Δ synthetic lethality was suppressed (Figure 2K). The viability of the *kss1*Δ *gcn5*Δ *rts1*Δ, and the

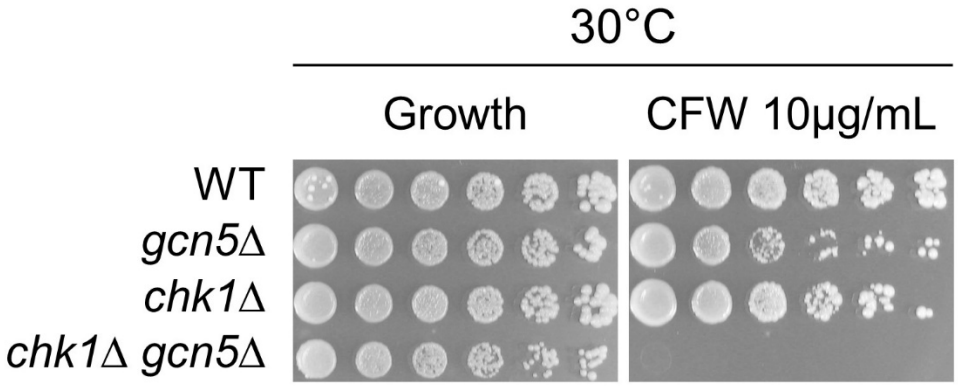

Figure 2H ***chk1*Δ rescues *gcn5*Δ calcofluor-white sensitivity.** Five-fold dilution of wild type (LPY 5), *gcn5*Δ (LPY 13319), *chk1*Δ (LPY 20086), and *chk1*Δ *gcn5*Δ (LPY 20298) were plated onto YPAD (growth) and calcofluor-white (CFW) plates with 10µg/ml concentration.

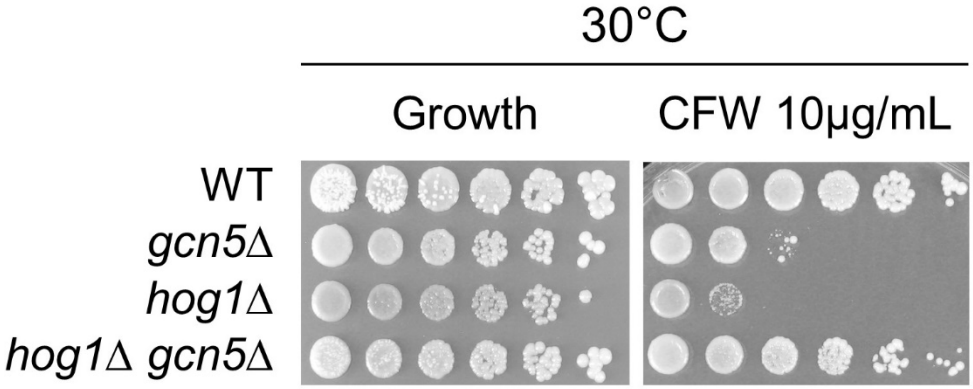

Figure 2I ***hog1*Δ rescues *gcn5*Δ calcofluor-white sensitivity.** Five-fold dilution of *wild type* (LPY 5), *gcn5*Δ (LPY 13319), *hog1*Δ (LPY 21374), and *hog1*Δ *gcn5*Δ (LPY 21366) were plated onto YPAD (growth) and calcofluor-white (CFW) plates with 10µg/ml concentration. *hog1*Δ and *gcn5*Δ single mutant showed CFW sensitivity while *hog1*Δ *gcn5*Δ shows resistance to CFW.

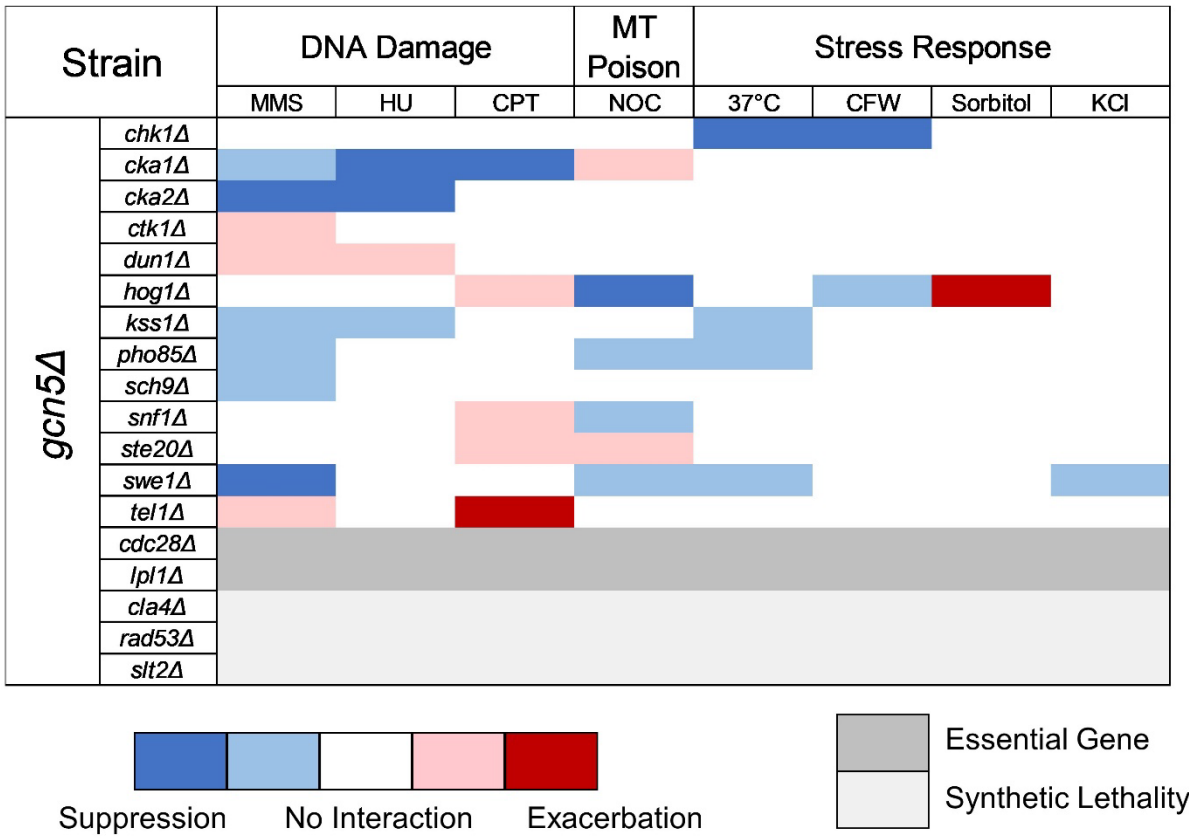

Figure 2J **Distinct patterns of phenotypic interaction with *gcn5*Δ were observed.** A heat map to summarize the screen results is shown. Semiquantitative dilution assays were performed with WT (LPY 5), *gcn5*Δ (LPY 13319), and the *gcn5*Δ *kinx*Δ mutant under a variety of stress conditions. The cells were scored after growth at 30°C for 3 days. A suppression of *gcn5*Δ phenotypes is shown as a blue cell in the heat map, with dark blue indicating strong suppression, and light blue indicating partial suppression. Exacerbation of *gcn5*Δ phenotypes is shown in red, with similar quantitative comparisons. When the *gcn5*Δ *kinx*Δ growth is comparable to *gcn5*Δ, a white cell is used to indicate no interaction. Grey and black cells denote essential gene deletions and gene deletions that cause synthetic lethality in *gcn5*Δ background, respectively. The non-essential kinase deletions are shown in alphabetical order.

*hog1*Δ *gcn5*Δ *rts1*Δ triple mutant indicates that both Kss1 and Hog1 are potentially involved in the *RTS1-GCN5* interaction.

Discussion:

Synthetic lethality screen identified previously reported and newly found lethal interaction with *gcn5*Δ

The Viability of *gcn5Δ kinxΔ* is a prerequisite for phenotypic analysis. The synthetic lethality screen eliminated kinase candidates that cause lethality in *gcn5*Δ mutants when deleted. Out of the 18 potential kinase mutations, we reported 13 viable kinase deletions in *gcn5*Δ mutants (Table 2.1). From the synthetic lethality screen, we confirmed previously observed lethal interaction between *gcn5*Δ and *cla4*Δ as well as *gcn5*Δ and *rad53*Δ (Cherry et al., 2012; Srivas et al., 2016). Furthermore, we also identified synthetic lethality caused by concurrent deletion of *SLT2* and *GCN5*. Slt2 is a MAPK modulating the cell wall integrity pathway (CWI) (Elion, 2003). Gcn5-containing SAGA complex was found to be involved in Slt2 mediated transcription of the cell wall stress-responsive gene (Sanz et al., 2016). Indeed, deletion of *GCN5* by itself already causes severe cell wall defects due to altered expression of genes involved in the synthesis of cellulose, a major component of yeast cell wall (Zheng et al., 2019). Therefore, the synthetic lethality between *gcn5*Δ and *slt2*Δ could be a consequence of a functionally compromised cell wall integrity pathway.

Kinase deletion results in unique patterns of suppression of *gcn5*Δ phenotypes

Previously, in Petty et al 2016, *RTS1* was identified as a dosage suppressor of various *gcn5*Δ phenotypes. *RTS1* overexpression rescues *gcn5*Δ temperature sensitivity, nocodazole sensitivity, and DNA damage sensitivity induced by HU and

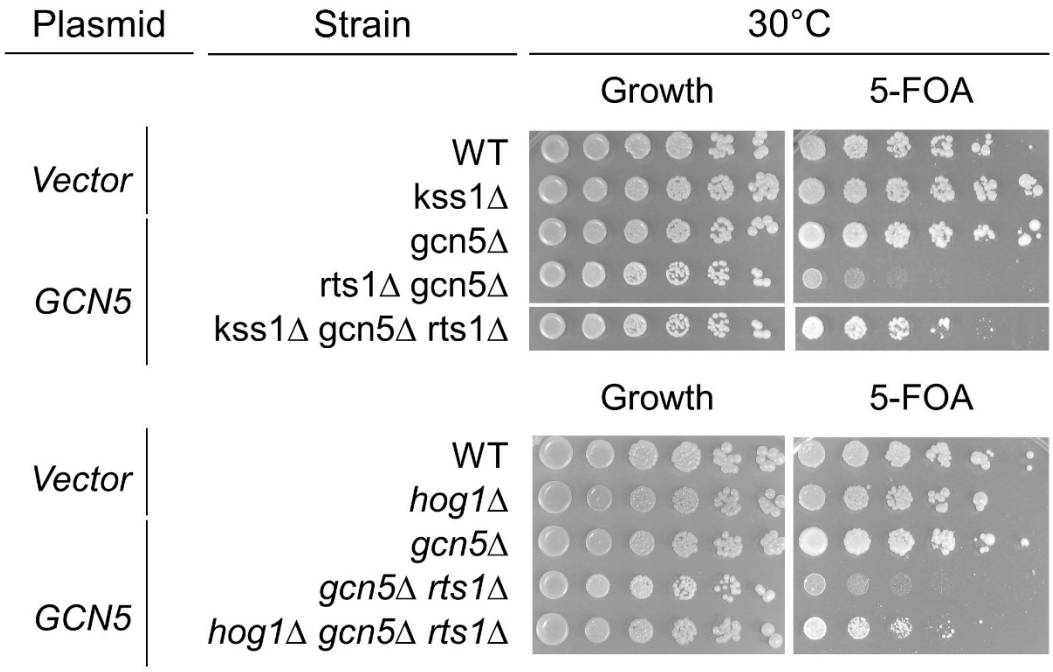

Figure 2K ***hog1*Δ and *kss1*Δ rescues *gcn5*Δ *rts1*Δ synthetic lethality.** The *hog1*Δ *gcn5*Δ *rts1*Δ and *hog1*Δ *gcn5*Δ *rts1*Δ triple mutant was constructed with a *CEN-URA3-GCN5 (*pLP 1640*)* covering plasmid or single mutants with vector controls, *CEN-URA3* vector (pLP 126) whereas WT*, hog1*Δ*,* and *kss1*Δ were transformed with a *CEN-URA3* vector (pLP 126) as controls. Five-fold dilutions of wildtype (LPY 5 + pLP 126), *hog1*Δ (LPY 21374 + pLP 126), *kss*Δ (LPY 1873 + pLP 126), *gcn5*Δ (LPY 13319 + pLP 1640)*, gcn5*Δ *rts1*Δ (LPY 15178 + pLP 1640), *hog1*Δ *gcn5*Δ *rts1*Δ (LPY 21388 + pLP 1640), and *hog1*Δ *gcn5*Δ *rts1*Δ (LPY 23189+pLP 1640) were plated onto URA- (growth) or 5-FOA plate to select against the *CEN-URA3-GCN5* plasmid and incubated at 30°C for three days.

MMS (Petty et al., 2016). In this study, we reported *chk1*Δ suppression of *gcn5*Δ temperature sensitivity at 37°C, *hog1*Δ rescue of *gcn5*Δ nocodazole sensitivity, *kss1*Δ suppression of *gcn5*Δ HU and MMS sensitivity. Contrary to *RTS1* overexpression which rescues a variety of *gcn5*Δ phenotypes, deletion of nuclear kinase only rescues a subset of phenotypes. We attribute the disparity to the difference in specificity between kinase and phosphatase. Compared to protein kinases, which shows higher substrate specificity, protein phosphatases normally have a broader specificity (Sparks & Brautigan, 1986). As a result, the nuclear kinase studied might be involved in a less broad range of biological processes compared to the protein phosphatase 2A (PP2A). Therefore, based on these findings, we concluded that multiple kinases might be involved in the *RTS1-GCN5*, each nuclear kinase might be involved in a distinct aspect of the *RTS1-GCN5* interaction.

GCN5 deletion causes severe sensitivity to high growth temperature at 37°C (Petty et al., 2016). In budding yeast, cell wall integrity pathway is closely linked to growth at an elevated temperature (Levin., 2005), and the HAT Gcn5 is required for response to cell wall damage (Xue-Franzén et al., 2010). Therefore, we hypothesized that the growth defect at high temperature in *gcn5*Δ mutants are partially caused by cell wall defects, which is further supported by the synthetic lethality of *gcn5*Δ *slt2*Δ double mutant. In this study, we reported that loss of the DNA Damage checkpoint kinase Chk1 rescues *gcn5*Δ temperature sensitivity at elevated growth temperature as well as *gcn5*Δ sensitivity to CFW, a chemical that induces cell wall stress. Together, these results suggest that the functional interaction between *CHK1* and *GCN5* may take place in the context of cell-wall integrity pathways. Further investigation of the *CHK1-GCN5*

interaction might elucidate the roles played by *CHK1* in growth under elevated temperature and the cell wall integrity pathway,

Loss of filamentous response MAPK Kss1 rescues *gcn5*Δ DNA Damage phenotypes:

In this study, we reported that loss of the MAPK governing filamentous growth response, Kss1, rescues *gcn5*Δ HU and MMS sensitivity in the *MATα* background. MMS is a DNA methylation agent that modifies the nucleotides guanine and adenine (Alvino et al., 2007); HU is an inhibitor of ribonucleotide reductase, a protein involved in the synthesis of deoxyribonucleotides: HU treatment causes alteration in dNTP pools (Alvino et al., 2007). Both hydroxyurea and MMS exert genotoxic stress during S-phase, causing replication fork stall, collapse, and eventually double-strand break (Alvino et al., 2007; Wyatt & Pittman, 2006). Our results suggest a previously unknown role for *KSS1-GCN5* interaction in the DNA Damage responses.

Furthermore, loss of *KSS1* was found to suppress the synthetic lethality interaction between *gcn5*Δ and *rts1*Δ (Figure 2.K), indicating that Kss1 is indeed involved in the *RTS1-GCN5* interaction. Therefore, we suspected that deletion of *KSS1* might also restore Gcn5-mediate histone acetylation in response to DNA damage. Further investigation of the *KSS1-RTS1-GCN5* interaction will help reveal the role played by Kss1 in the DNA damage response as well as the significance of histone modification crosstalk between acetylation and phosphorylation in the DNA damage response.

Loss of osmotic stress response MAPK Hog1 rescues *gcn5*Δ cell cycle phenotypes:

In this study, we reported that the loss of the MAPK governing hyperosmotic stress response, Hog1, rescues *gcn5*Δ sensitivity to nocodazole, a microtubule poison.

A proper cell cycle arrest is crucial to the survival of cells under hyperosmotic stress; upon hyperosmotic stress, Hog1 is capable of mediating arrest at various stages of the cell cycle (Clotet et al., 2006; Escoté et al., 2004; Yaakov et al., 2009). However, though the role of Hog1 in cell cycle progression under hyperosmotic stress is well documented, little is known about the effect of Hog1 on the cell cycle progression under non-stressed conditions. Our results suggest a previously unknown role for Hog1 in the cell cycle progression of non-stressed cells.

Furthermore, suppression of the *gcn5*Δ *rts1*Δ synthetic lethality was observed in *gcn5*Δ *rts1*Δ *hog1*Δ triple mutant, indicating a role for Hog1 in the *RTS1-GCN5* nexus. The *HOG1-GCN5* interaction is a topic of interest because the investigation of the *GCN5-RTS1* interaction in the context of chromosome segregation revealed that Sgo1-mediated Rts1 localization to the centromere region is crucial for the dosage-dependent rescue of *gcn5Δ* chromosome segregation phenotypes (Petty et al., 2018). Furthermore, two phosphorylatable serine residues on the centromeric specific H3 histone variant Cse4, Cse4-S180 and Cse4-S135 were identified to be involved in the *RTS1-GCN5* interaction (Petty et al., 2018). Based on the previous finding, we suspected that loss of *HOG1* might be involved in the *RTS1-GCN5* interaction in the context of chromosome segregation: dynamic phosphorylation mediated by Hog1 and $PP2A^{Rts1}$ on the residues of the centromeric specific histone Ces4 potentially contributes to the spindle assembly checkpoint and chromosome segregation function in *gcn5Δ* mutants

Chapter 2, in part is currently being prepared for submission for publication of the material. Liu, Qihao; Petty, Emily; Pillus, Lorraine. The thesis author was the primary investigator and author of this material.

Chapter 3: H2B threonine 91 is required for *hog1Δ* rescue of *gcn5Δ* nocodazole sensitivity

Introduction:

In chapter 2, we have established that the deletion of *HOG1* MAPK in the *gcn5*Δ background results in a specific increase in nocodazole resistance. Furthermore, *hog1*Δ was found to suppress *gcn5*Δ *rts1*Δ synthetic lethality, indicating a role for Hog1 in the Rts1-Gcn5 interaction. Previous studies have identified phosphorylatable histone residues on histone H2B to be involved in the *RTS1-GCN5* interaction (Petty et al., 2016). Whereas the phosphodeficient *htb1-T91A* mutant hinders the rescue of *gcn5Δ* phenotypes by *RTS1* overexpression, the phosphomimic *htb1-T91D* mutation causes lethality, indicating that the dynamic phosphorylation of histone H2B-T91 is crucial for the dosage suppression of *gcn5*Δ phenotypes by *RTS1*.

Furthermore, deletion of *GCN5* was found to abolish the centromeric localization of Rts1 during spindle assembly checkpoint for proper tension sensing during mitosis (Petty et al., 2018). Overexpression of *RTS1* restores the centromeric localization of Rts1, resulting in the suppression of *gcn5*Δ nocodazole sensitivity. A previous study identified phosphorylatable residue on the centromeric specific histone Cse4, Cse4-S180, which plays a role in Rts1 centromeric localization. Phosphodeficient mutation *cse4-S180A* restores Rts1 centromeric localization whereas the phosphomimetic mutation *cse4-S180EE* causes lethality in *gcn5Δ* (Petty et al., 2018). Together, these results suggest that Cse4-S180 residue plays a crucial role in the *RTS1-GCN5* interaction in the context of chromosome segregation, and the tightly regulated dynamic phosphorylation on Cse4 residues is crucial for proper cellular response to

nocodazole. Since Loss of *HOG1* was found to specifically suppress *gcn5*Δ nocodazole sensitivity, we hypothesized that Hog1 might be involved in the Rts1-Gcn5 interaction in the context of the spindle assembly checkpoint.

In the previous chapter, we have established *hog1Δ* as a suppressor mutation that improves *gcn5Δ* sensitivity to nocodazole, which induces chromosome segregation defect. The loss of Hog1 rescues the synthetic lethality of the *gcn5*Δ *rts1*Δ mutant. In this chapter, we aim to determine if the loss of Hog1's catalytic activity provides an underlying mechanism for the *HOG1-GCN5* interaction. Furthermore, the roles of histone residues H2B-T91, Cse4-S180, and Cse4-S135 in the *HOG1-GCN5* interaction were determined.

Results:

Loss of Hog1 catalytic activity rescues *gcn5*Δ nocodazole sensitivity

Previously, we have established that deletion of *HOG1* significantly improves the growth of *gcn5*Δ mutants under microtubule destabilizing conditions (Figure 2F). We tested if loss of the catalytic activity of Hog1 is the factor that underlies the rescue. The catalytically inactive Hog1 mutant was constructed by replacing the threonine 174 residue on the Hog1 activation loop with alanine via CRISPR-based mutagenesis. The *hog1-T174A* mutation prevents the activation of Hog1 catalytic activity by the upstream MAPKK (Maayan et al., 2012; Maeda et al., 1995) (Figure 3A). The *hog1-T174A gcn5*Δ double mutant was constructed genetically and tested for growth on nocodazole. Indeed, loss of Hog1 catalytic activity is sufficient to restore growth in the *gcn5Δ* background upon the nocodazole challenge (Figure 3B). Further, loss of Hog1 catalytic activity improves nocodazole resistance not only in *gcn5*Δ mutants but also in wildtype

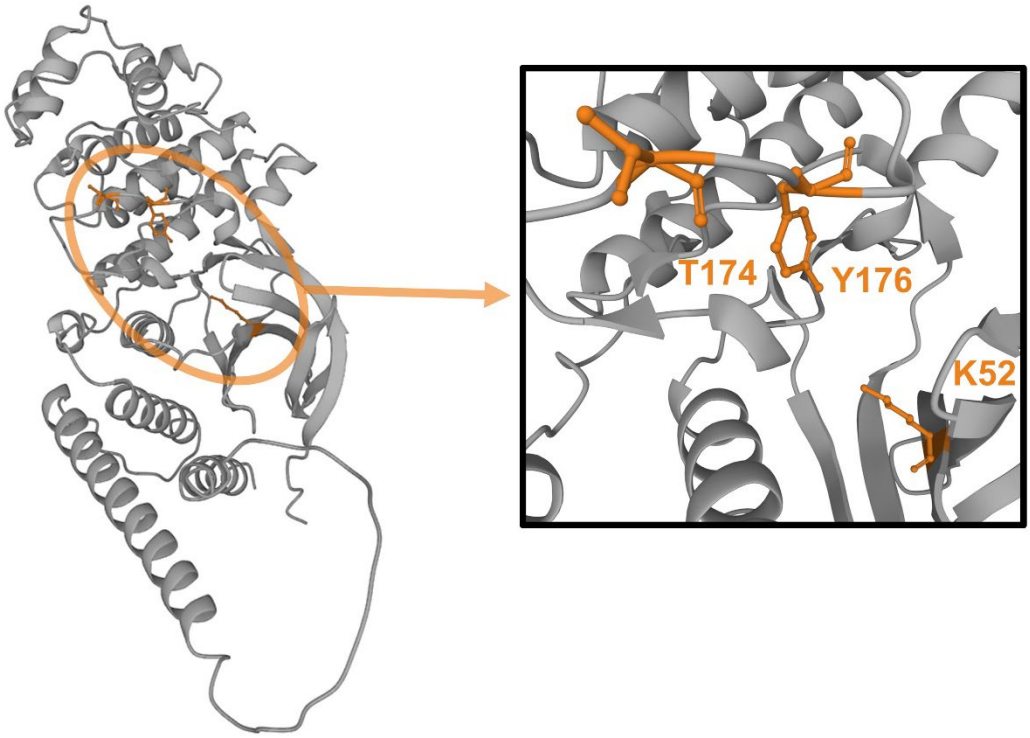

Figure 3A ***Saccharomyces cerevisiae* Hog1 protein structure.** Shown here is the Hog1 protein structure obtained from Alphafold (https://alphafold.ebi.ac.uk/entry/P32485). Hog1 catalytic residue R52 and activation loop residue T174 and Y176 are labeled dark pink.

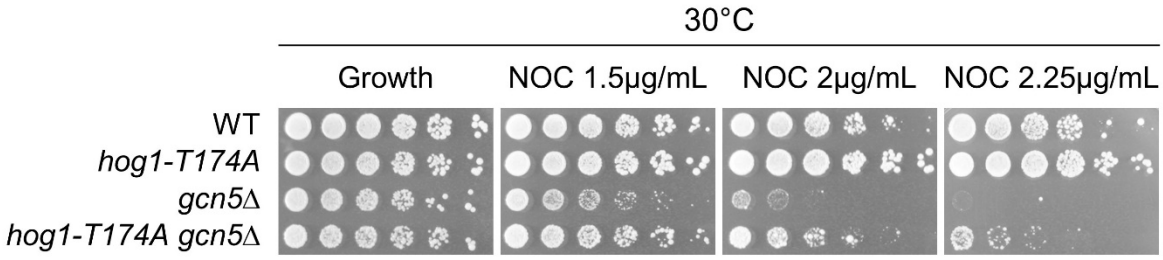

Figure 3B ***hog1-T174A* rescues *gcn5*Δ nocodazole sensitivity.** Five-fold dilution of WT (LPY 5), *gcn5*Δ (LPY 13319), *hog1-T174A* (LPY 23147) *and hog1-T174A gcn5*Δ (LPY 23150) were plated onto YPAD (growth) and nocodazole (NOC) media with varying concentration. *hog1-T174A gcn5*Δ showed concentration-independent suppression of *gcn5*Δ sensitivity to Nocodazole. On higher nocodazole concentration (>2µg/mL) an increase in the *hog1-T174A* nocodazole resistance was observed.

(WT) cells (Figure 3B). These results suggest that loss of Hog1 kinase activity may generally reduce nocodazole sensitivity.

Loss of Hog1 catalytic activity rescues *gcn5*Δ *rts1*Δ synthetic lethality

Concurrent loss of Gcn5 and Rts1 induces synthetic lethality (Petty et al., 2016). We tested if loss of Hog1 kinase activity provided the specific mechanism for the rescue of *rts1Δ gcn5Δ* synthetic lethality. In this case, the *CEN-HIS3-hog1-T174A* plasmid was transformed into the *CEN-URA3-GCN5*-bearing *hog1Δ rts1Δ gcn5Δ* strain. The *hog1Δ rts1Δ gcn5Δ* strain showed growth comparable to WT on the 5-FOA medium, indicating that the catalytic inactivation of *HOG1* is what drives suppression of the *rts1Δ gcn5Δ* synthetic lethality (Figure 3C). Further, the *hog1Δ rts1Δ gcn5Δ* mutant bearing the *CEN-HIS3-HOG1* plasmid showed compromised growth upon loss of the *CEN-URA3-GCN5* plasmid (Figure 3D). Together, these results support the idea that loss of Hog1's catalytic activity, and not some other property of the enzyme, is what rescues *rts1Δ gcn5Δ* synthetic lethality, pointing to a key enzymatic role in the Rts1-Gcn5 interaction.

Phosphodeficient *htb1-T91A* mutation attenuates *hog1*Δ rescue of *gcn5*Δ nocodazole sensitivity

Previously we established that dynamic phosphorylation on H2B-T91 plays an important role in the Gcn5-Rts1 interaction, in that the phosphodeficient *htb1-T91A* mutant hinders *RTS1* dosage-dependent rescue of *gcn5Δ* phenotypes (Petty et al., 2016). We tested if the same histone residue is involved in the Gcn5-Hog1 interaction. Confirming previous observations, we found that *htb1-T91D/E* phosphomimetic mutations cause lethality in all backgrounds (Figure 3E). The *htb1-T91A* allele was found to hinder the growth of *hog1Δ gcn5Δ* on nocodazole-containing media,

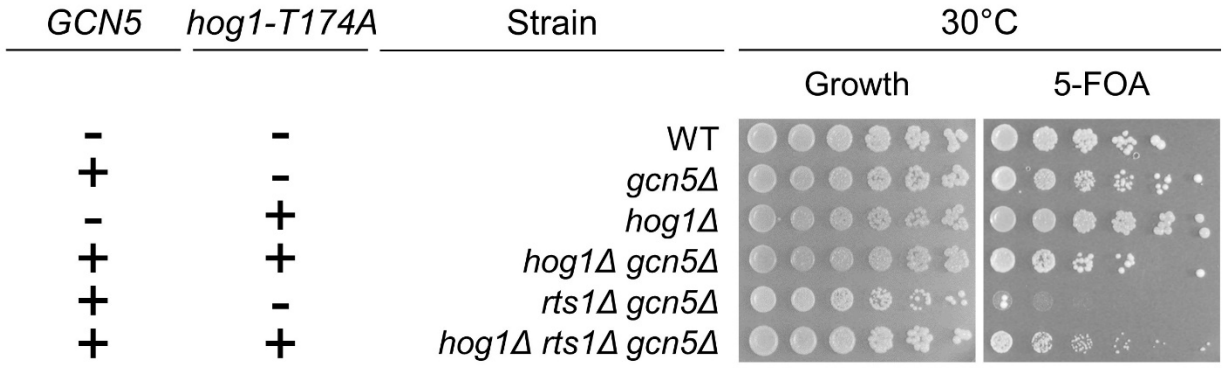

Figure 3C **Deletion of *HOG1* or loss of Hog1 catalytic activity rescues *gcn5*Δ *rts1*Δ synthetic lethality.** Wildtype (LPY 5), *hog1*Δ (LPY 21374), *gcn5*Δ (LPY 13319), *hog1*Δ *gcn5*Δ (LPY 21366), *gcn5*Δ *rts1*Δ (LPY 15178), and *hog1*Δ *gcn5*Δ *rts1*Δ (LPY 21388) containing either the *CEN-URA-GCN5* (pLP 1640) covering plasmid, or the *CEN-URA3-vector* (pLP 126) was transformed with either the *CEN-HIS3-hog1-T174A* plasmid or the *CEN-HIS3-vector*. Strains were plated onto URA-HIS- (growth) and HIS- 5-FOA plate to select against the *CEN-URA3-GCN5* plasmid. Cells were incubated at 30°C for three days. The *hog1*Δ *gcn5*Δ *rts1*Δ triple mutant containing the *CEN-HIS3-hog1-T174A* showed growth on 5-FOA medium, indicating that loss of Hog1 catalytic activity suppresses *gcn5*Δ *rts1*Δ synthetic lethality.

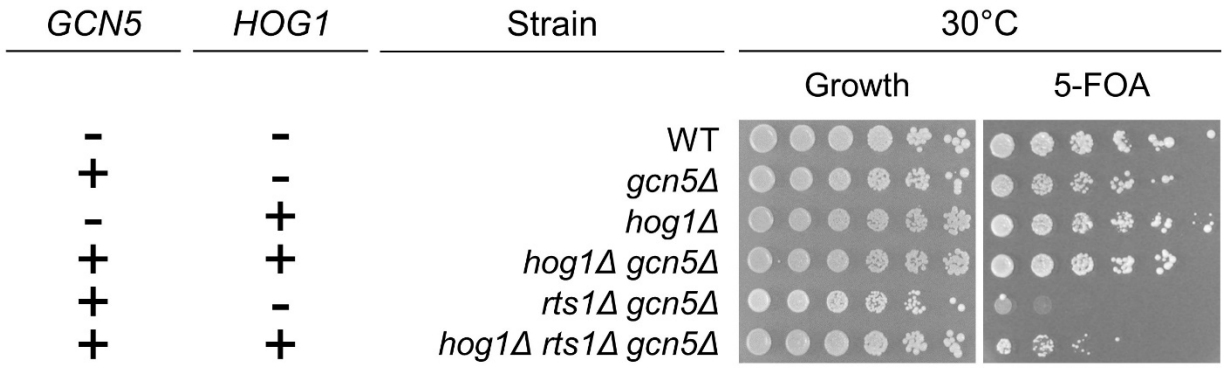

Figure 3D **WT-*HOG1* gene restores synthetic sickness in the *hog1Δ rts1Δ gcn5Δ* strain.** The *CEN-HIS3-HOG1* plasmid or the *CEN-HIS3-vector* control were transformed into wildtype (LPY 5), *hog1*Δ (LPY 21374), *gcn5*Δ (LPY 13319), *hog1*Δ *gcn5*Δ (LPY 21366), *gcn5*Δ *rts1*Δ (LPY 15178), and *hog1*Δ *gcn5*Δ *rts1*Δ (LPY 21388) containing either the *CEN-URA-GCN5* (pLP 1640) covering plasmid, or the *CEN-URA3-vector* (pLP 126). Transformants were plated onto URA-HIS- (growth) and HIS- 5-FOA and incubated at 30°C for three days. The *hog1*Δ *gcn5*Δ *rts1*Δ triple mutant containing the *CEN-HIS3-HOG1* showed reduced growth compared to the triple mutant containing the *CEN-HIS3-vector*.

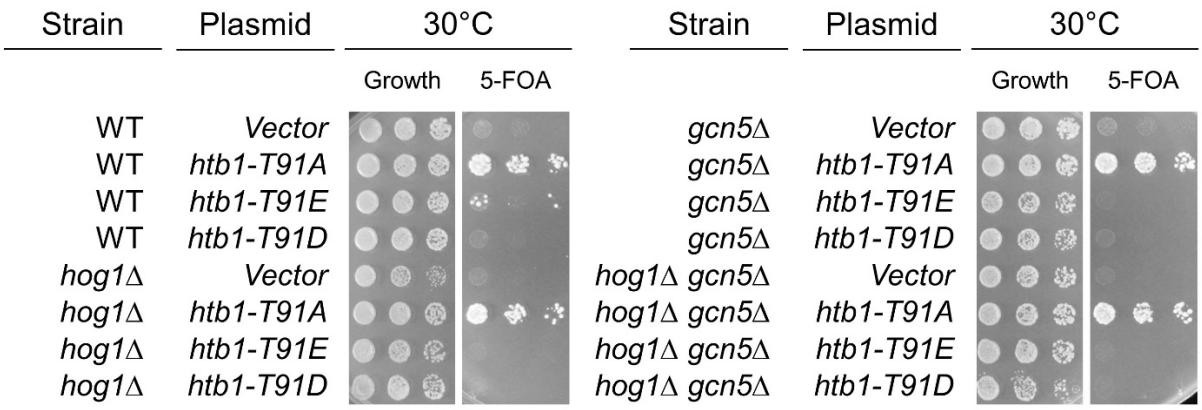

Figure 3E **Phosphomimetic *htb1-T91E/D* mutation induce lethality in *hog1*Δ *gcn5*Δ background.** *hog1*Δ *gcn5*Δ strain lacking genes encoding the canonical histones were constructed and covered with a URA3 plasmid carrying WT histone genes. Histone plasmids carrying the *htb1-T91* mutations marked with HIS3 marker was then transformed into the histone shuffle *hog1*Δ *gcn5*Δ strain. The strains were maintained on URA-HIS- plate to retain version of the histone plasmid. To test for synthetic lethality, the strains were plated on to URA-HIS- (growth) and 5-FOA. Growth on 5-FOA plates indicates that the histone mutation was viable in each background.

indicating that the phosphodeficient histone mutation partially abolishes the *hog1Δ* rescue of *gcn5Δ* sensitivity to nocodazole (Figure 3F). Moderate rescue of *gcn5Δ* sensitivity to nocodazole remains in the *hog1*Δ *gcn5*Δ *htb1-T91A* strain at lower nocodazole concentrations (Figure 3F). Together, these results confirmed that mutation of histone H2B-T91 exerts an effect on the Hog1-Gcn5 interaction, indicating that the phosphorylatable H2B-T91 residue plays an important role in the Hog1-Gcn5 interaction. Both Gcn5-Rts1 (Petty et al., 2016) and Gcn5-Hog1 (this study) functional interactions rely on H2B-T91, further supporting the hypothesis that Hog1 and $PP2A^{Rts1}$ together mediate dynamic histone modifications crucial for *gcn5Δ* mutant.

cse4-S180A and *cse4-S135A* do not hinder Hog1 rescue of *gcn5*Δ nocodazole sensitivity

Beyond the canonical core histones, residues have been identified in the centromeric specific histone Cse4 that hinder *RTS1* dosage-dependent suppression of *gcn5Δ* DNA damage sensitivity but improve *gcn5Δ* resistance to nocodazole (Petty et al., 2018). Therefore, the effects of these, *cse4-S180A* and *cse4-S135A*, were tested in *hog1Δ gcn5Δ* mutants. Strains of *hog1Δ gcn5Δ* containing the integrated *cse4-S180A, cse4-S135A* alleles, or WT *CSE4* were constructed and plated onto nocodazole-containing media. No difference was observed between the growth of the *hog1*Δ *gcn5*Δ *cse4-S135A*, *hog1*Δ *gcn5*Δ *cse4-S180A,* and *hog1*Δ *gcn5*Δ *CSE4* strains (Figure 3G). Thus, we concluded that phosphodeficient *cse4* alleles do not negatively affect the Hog1-Gcn5 interaction.

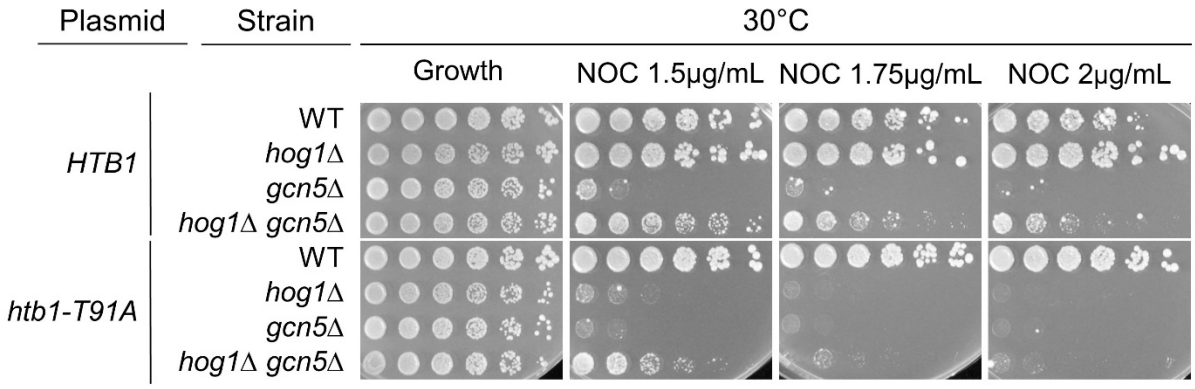

Figure 3F **Phosphodeficient *htb1-T91A* mutation attenuates *hog1*Δ rescue of *gcn5*Δ nocodazole sensitivity.** Viable *htb1-T91A* mutants recovered from previous synthetic lethality tests were plated onto YPAD (growth) and nocodazole plates with varying concentration. The strains were allowed to grow at 30 °C for 3 days.

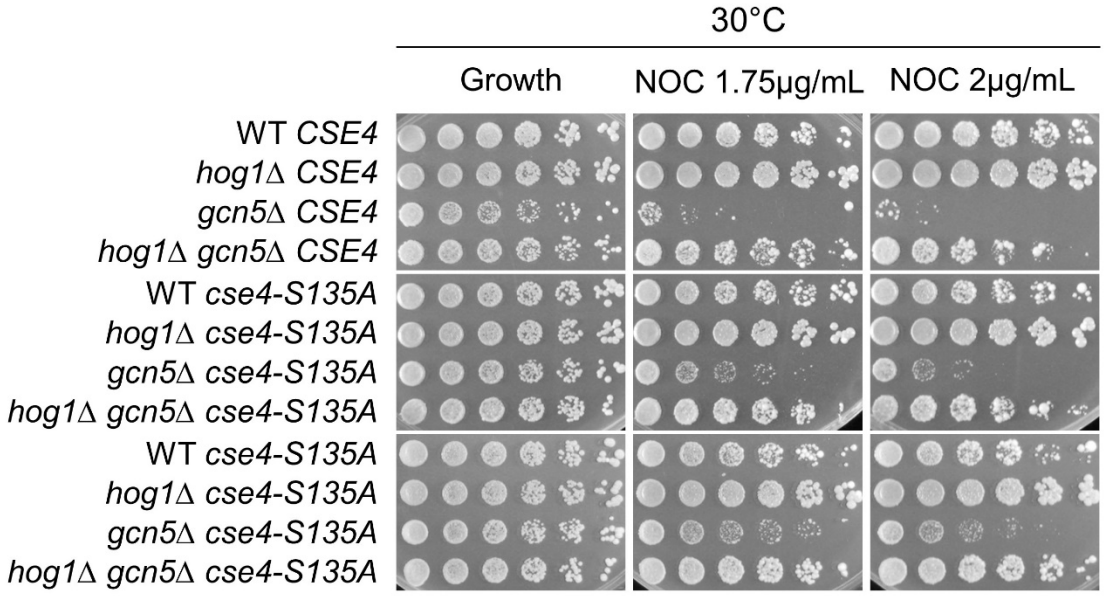

Figure 3G ***cse4-S180A* and *cse4-S135A* mutation does not hinder *hog1*Δ rescue *gcn5*Δ nocodazole sensitivity.** *hog1*Δ *gcn5*Δ *cse4-S135A, hog1*Δ *gcn5*Δ *cse4-S180A, and hog1*Δ *gcn5*Δ *CSE4* were constructed and plated onto YPAD (growth) and nocodazole plate with varying concentrations. The strains were allowed to grow at 30 °C for 3 days

Discussion:

A Role for Hog1 in the Gn5-PP2A Rts1 Nexus

The results show that Hog1 plays a part in the Gcn5-Rts1 interaction in microtubule destabilizing conditions. To determine if phosphorylatable histone residues might be required in the Hog1-Gcn5 interaction, we focused on H2B-T91, previously found to be involved in the Rts1-Gcn5 interaction. In the *gcn5Δ hog1Δ* mutant, we discovered that the phosphodeficient *htb-T91A* mutation dampens the suppression of *gcn5Δ* sensitivity to nocodazole by *hog1Δ* (Figure 3B). These results are consistent with joint roles for Hog1 and $PP2A^{Rts1}$ in mediating dynamic phosphorylation on H2B-T91, which is crucial for the survival of *gcn5*Δ mutants.

We note that the sequence surrounding H2B-T91 does not match the established Hog1 phosphorylation consensus, which ordinarily contains a serine or a threonine preceding a proline residue (Mok et al., 2010). Thus, it seems that dynamic phosphorylation of H2B-T91 via activation of another nuclear kinase may be the target of Hog1. Indeed, H2B-T91 in yeast has been predicted as a target of Ste20, a member of the p21-activated kinase family (Petty et al., 2016, Wang et al., 2020). Ste20 was already found to mediate histone phosphorylation involved in various cellular processes. Ste20-mediated H2B-S10 phosphorylation was found to depend on the dephosphorylation of Hos3 on H2B-K11 (Ahn et al., 2005). Furthermore, Ste20-mediated phosphorylation of H4-S47 plays a role in the modulation of osmotic stress-responsive genes (Viéitez et al., 2020). Previous studies have shown that Ste20 interacts with Hog1 by regulating the activation of Hog1 in response to osmotic stress (O'Rourke & Herskowitz, 2002; Raitt et al., 2000). Therefore, we hypothesize that Hog1

potentially facilitates histone phosphorylation by Ste20. Deletion of Hog1 would thereby lead to loss of Ste20 mediated histone phosphorylation, restoring the phosphorylation balance vital for the *gcn5*∆ mutant. However, in this study, loss of *STE20* has been found to exacerbate *gcn5Δ* sensitivity to nocodazole (Figure 2J), indicating that such a simple hypothesis does not capture the functional relationship between Hog1, Gcn5, and Ste20.

Hog1 and $PP2A^{Rts1}$ might interact with different target in the context of spindle assembly checkpoint

Previous studies have found that Gcn5 plays an important role in the centromeric localization of Rts1, which in turn promotes the tension sensing function of the spindle assembly checkpoint (Petty et al., 2018). Since the loss of *HOG1* suppresses *gcn5Δ* nocodazole sensitivity as well as the synthetically lethal interaction with *rts1Δ*, we hypothesized that both *HOG1-GCN5* and *RTS1-GCN5* interactions involve the same residue on the centromeric specific histone Cse4. Results showed that mutation on Cse4 does not affect the *GCN5-HOG1* interaction, indicating that *HOG1-GCN5* and *RTS1-GCN5* interactions might require different substrates. Furthermore, neither Cse4-S180 or Cse4-S135 contains the phosphorylation consensus of Hog1. However, A single threonine residue, Cse4-T133, agrees with the phosphorylation consensus of Hog1. Therefore, we suspect that Hog1 and $PP2A^{Rts1}$ might function upon distinct targets to restore *gcn5Δ* nocodazole sensitivity.

Chapter 3, in part is currently being prepared for submission for publication of the material. Liu, Qihao; Petty, Emily; Pillus, Lorraine. The thesis author was the primary investigator and author of this material.

Chapter 4: *hog1Δ* specifically restores *gcn5Δ* viability in response to nocodazole

Introduction:

Cell Cycle is Controlled by Well-orchestrated Molecular Events:

The cell cycle is a process during which the generation and division of the genetic and cellular material produce two identical daughter cells from a single mother cell. The cell cycle of *S. cerevisiae* is composed of four phases: the G1 phase when the cell grows to appropriate sizes, the S phase, when the cell duplicates the genetic material, the G2 phase, when the cell prepares for cell division, and the M phase, when cell division takes place (Figure 4A). The orchestrated coordination between the oscillatory expression of cell cycle cyclin proteins Cln3, Cln1, Cln2, Clb5, Clb6, Clb2, and the cell-cycle dependent kinase (CDK) promotes the progression of the cell cycle. The *S. cerevisiae* cell cycle is governed by a single CDK known as Cdc28 (Lew and Reed, 1993). During each stage of the cell cycle, Cdc28 forms complexes with the timely expressed cyclin. Association of Cdc28 with cyclin alters the activity of the CDK, allowing the CDK to phosphorylate the correct substrate, coordinate the necessary cellular event, and advance cell cycle progression.

The proper monitoring and regulation of the cell cycle are crucial for the survival of the cells. Checkpoints between the key stages of the cell cycle offer a control mechanism that surveils the appropriate cell cycle progression (Hartwell & Weinert, 1989). In *S. cerevisiae*, the budding cycle and the nuclear cell cycle are closely related (Lew, 2003), allowing the morphogenesis checkpoint to control cell cycle progression by monitoring the yeast budding cycle. The morphogenesis checkpoint monitors the integrity of the actin cytoskeleton, which plays a crucial role during the polarized growth

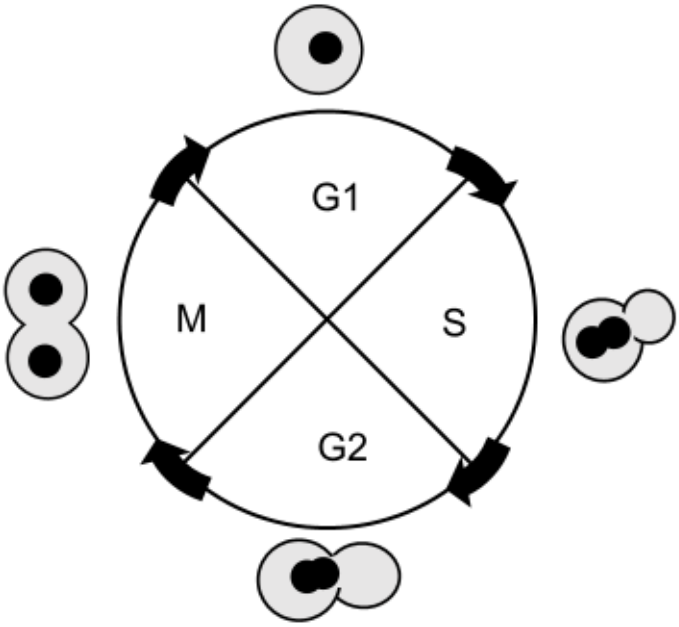

Figure 4A **Yeast cell cycle is closely related to bud morphological change**
The cell cycle of *S. cerevisiae* is composed of four phases: G1, S, G2, and M phase. Progression of cell cycle is controlled by well-orchestrated molecular events between cyclins and cell cycle dependent kinase (CDK)

necessary for budding, and the septin-based ring at the bud neck, which is essential for the division of the cells (McMillan et al., 1998; Cid et al., 2001; McMurray et al., 2011). The key component of the morphogenesis checkpoint is the CDK-inhibitory tyrosine kinase Swe1. Cdc28 association with Clb1-4 cyclins is required for the entry into mitosis (Mendenhall et al., 1998). The kinase Swe1 phosphorylates a single tyrosine residue Cdc28-Y19 to inhibit the kinase activity of Cdc28 and blocks entry into mitosis (Mendenhall et al., 1998). The localization and degradation of Swe1 are dependent on the Nim1-related protein kinase Hsl1 and protein arginine methyltransferase Hsl7 (Cid et al., 2001). Under normal conditions, Hsl1 and Hsl7 localize to the bud neck (Barral et al., 1999; Shulewitz et al., 1999), and the association of Hsl1 and Hsl7 promotes the proper localization and degradation of Swe1 at the bud neck, alleviating the inhibitory effect imposed on the CDK by Swe1, and signaling entry into mitosis (Asano et al., 2005, Cid et al., 2001). When the bud formation is disrupted by defects in septin ring assembly, Swe1 is stabilized at the bud neck (Shulewitz et al., 1999); therefore, imposing a prolonged arrest on the G2 stage of the cell cycle.It has been observed that deletion of either *HSL1* or *HSL7* is lethal in the *gcn5Δ* background (Ruault & Pillus, 2006). Deletion of the cyclin-dependent kinase inhibitor Swe1 alleviates the synthetic lethality in *gcn5Δ hsl1Δ* and *gcn5Δ hsl7Δ,* indicating that constitutive activation of the morphogenesis checkpoint is lethal in the *gcn5Δ* background.

Another crucial checkpoint that occurs during mitosis is the spindle assembly checkpoint. The spindle assembly checkpoint ensures faithful segregation of chromosomes and prevention of aneuploidy by monitoring the association of microtubule spindles and the kinetochore. Sgo1, a component of the spindle assembly

checkpoint, plays a crucial role in the process of chromosome segregation (Cherry et al., 2012 ; Nerusheva et al., 2014). In *S. cerevisiae*, Sgo1 contributes to the maintenance of the Aurora B kinase Ipl1 at the kinetochore, a key kinase whose catalytic activity disrupts the erroneous association between microtubule and kinetochore, ensuring the spindle fibers are correctly attached to the kinetochore prior to segregation (Peplowska et al., 2014). Furthermore, Sgo1 also contributes to the centromeric localization of Rts1 (Peplowska et al., 2014) which plays a significant role in the correct orientation and segregation of the sister chromatids into the daughter cells.

In *S. cerevisiae*, anaphase onset and mitotic exit follow the faithful segregation of sister chromatids. The mitotic exit network (MEN) controls the mitotic exit and cytokinesis by coordinating molecular events resulting in the inactivation of cyclin-dependent kinase (CDK), reversal of CDK-mediated phosphorylation, accumulation of CDK inhibitors, and promotion of cyclin destruction (Campbell et al., 2019; Jin et al., 2008; Visintin et al., 1998). Under conditions where the kinetochore-microtubule attachment is destabilized, proper MEN inhibition is required for appropriate spindle assembly checkpoint (SAC) function to ensure correct orientation and segregation of sister chromatids (Caydasi et al., 2010).

Chromatin Modifying Enzyme Gcn5 is Involved in Cell Cycle Progression and Checkpoints:

Since histones are crucial in the compaction and organization of genetic materials, the histone genes are tightly regulated and expressed during the cell cycle (Eriksson et al., 2012). Deletion of *GCN5*, a gene encoding histone acetyltransferase involved in multiple cellular processes, negatively affects the histone gene expression

(Huisinga & Pugh, 2004). Furthermore, Cells lacking Gcn5 also show a variety of cell-cycle related phenotypes such as the sensitivity to the microtubule destabilizer nocodazole (Petty et al., 2016), the slow progression through the G1/S phase transition (Petty et al. 2016), and the slow progression through the G2/M transition (Howe et al., 2001; Petty et al., 2018). Previously, we reported that the overexpression of *RTS1*, a regulatory subunit of protein phosphatase 2A, rescues the cell-cycle related phenotypes of *gcn5Δ* cells. Loss of *GCN5* results in the loss of Rts1 centromeric localization, which is crucial for the proper execution of the spindle assembly checkpoint. Overexpression of *RTS1* restores such localization, thus rescuing *gcn5Δ* sensitivity to nocodazole. Furthermore, the unphosphorylatable mutant *cse4-S180A*, and *cse4-S135A* both rescue *gcn5Δ* nocodazole sensitivity. Additionally, *cse4-S180A* further restores Rts1 centromeric localization in *gcn5Δ* cells (Petty et al., 2018). Together, these results suggest that key histone residues that can undergo dynamic phosphorylation are involved in the *RTS1-GCN5* interaction in the context of chromosome segregation.

Hog1 Controls Cell Cycle Progression to Elicit Appropriate Stress Response:

When the cells are under osmotic stress, the abilities to initiate appropriate cellular responses and to temporarily pause cell cycle progression are essential for the survival and proliferation of the cells. Hog1, the MAPK that transmits extracellular osmotic stress signals to intracellular responses, halts and resumes the cell cycle at various stages to ensure appropriate stress responses. During the G1/S phase transition, Hog1 induces cell cycle arrest by stabilizing the cyclin-dependent kinase inhibitor Sic1 (Escoté et al., 2004); furthermore, Hog1 hinders the S phase progression via phosphorylation of the key components of DNA polymerase, allowing appropriate

osmotic stress-induced gene expression prior to the replication of genetic material (Yaakov et al., 2009). Hog1 achieves the G2/M arrest via phosphorylation of the morphogenesis checkpoint components Hsl1, which contributes to Hsl7 delocalization from the bud neck and eventually the stabilization of Swe1 (Clotet et al., 2006). When osmotic stress is presented during mitosis, Hog1 delays mitotic exit by downregulating the interaction between the nucleolar protein Net1 and the phosphatase Cdc14 which is essential for mitotic exit (Jiménez et al., 2020). Overall, Hog1 exerts comprehensive control over the progression of the cell cycle to ensure proper stress response.

Beyond the involvement of Hog1 in cell cycle progression under osmotic stress, a previous study performed by Pigula et al also implies that Hog1 might be involved in cell cycle progression through an unknown mechanism. The study reported that deletion of *HOG1* under normal conditions delays the spindle disassembly process, which is crucial for proper mitotic exit (Pigula et al., 2014). Reiser et al. reported that sustained activation of *HOG1* rescues the mitotic exit defects in MEN mutants (Reiser et al., 2006). These studies imply that the involvement of Hog1 in cell cycle progression might extend beyond osmotic stress response.

Since the *S. cerevisiae* cell cycle is closely related to the budding cycle, cell-cycle related phenotypes of *gcn5Δ* and *hog1Δ gcn5Δ* were investigated via budding indexes and then closely analyzed via flow cytometry for genetic content. In this chapter, further investigation into the *HOG1-GCN5* interaction is conducted in the context of cell cycle progression. Semiquantitative growth assay and 5-FOA counter-selection are used to test for the rescue of *gcn5Δ hsl1Δ* and *gcn5Δ hsl7Δ* synthetic lethality by *hog1Δ*.

Results:

HOG1 deletion does not rescue *gcn5Δ* budding defects or cell cycle defects in asynchronous and synchronous cell cultures

RTS1 overexpression restores *gcn5Δ* cell cycle progression at both the G1/S transition and the transition between mitosis and G1 (Petty et al., 2016, 2018). Considering Hog1 as a new player in the Rts1-Gcn5 interaction, we hypothesized that *hog1Δ* rescues the *gcn5Δ* sensitivity to nocodazole via improving cell cycle progression. To test this possibility, asynchronous cell cultures of *gcn5Δ* and *hog1Δ gcn5Δ* were incubated overnight and diluted back to 0.1 OD_{600} with fresh media and monitored after the resumption of exponential growth. The DNA content of these cell populations was evaluated via flow cytometry of propidium iodide-stained cells (Figure 4B). Both *gcn5Δ* and *hog1Δ gcn5Δ* show an increased G2/M population compared to the WT (Figure 4C), indicating that under normal growth conditions, both *gcn5Δ* and *hog1Δ gcn5Δ* have defective cell cycle progression.

In *S. cerevisiae* the budding cycle is directly related to the cell cycle (Zettel et al., 2003) (Figure 4.A), so we also microscopically evaluated the budding index to determine the percentage of each cell type in asynchronous cell cultures. In WT cultures, the cells with no buds, small buds, and large buds are found at approximately 50%, 25%, and 25% of the total population (Figure 4C). Only a small fraction of the WT population showed elongated (1%) or abnormal buds (1.2%). Compared to the WT, *gcn5Δ* and *hog1Δ gcn5Δ* cultures contained an increased proportion of elongated buds 24.0% and 22.4%) and decreased numbers of small and large buds (Figure 4C), indicating that these two mutants exhibit similar budding defects in growing populations

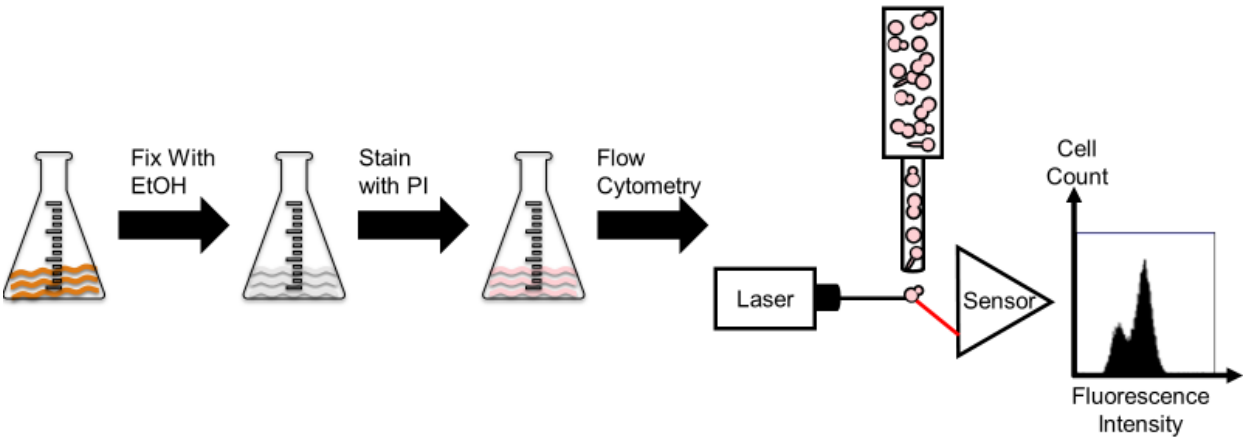

Figure 4B **Flow cytometry allows analysis of genetic content in a given cell population**. Log-phase cultures were grown to appropriate density, fixed with ethanol. The genetic content is then stained with fluorescent chemical propidium iodide.

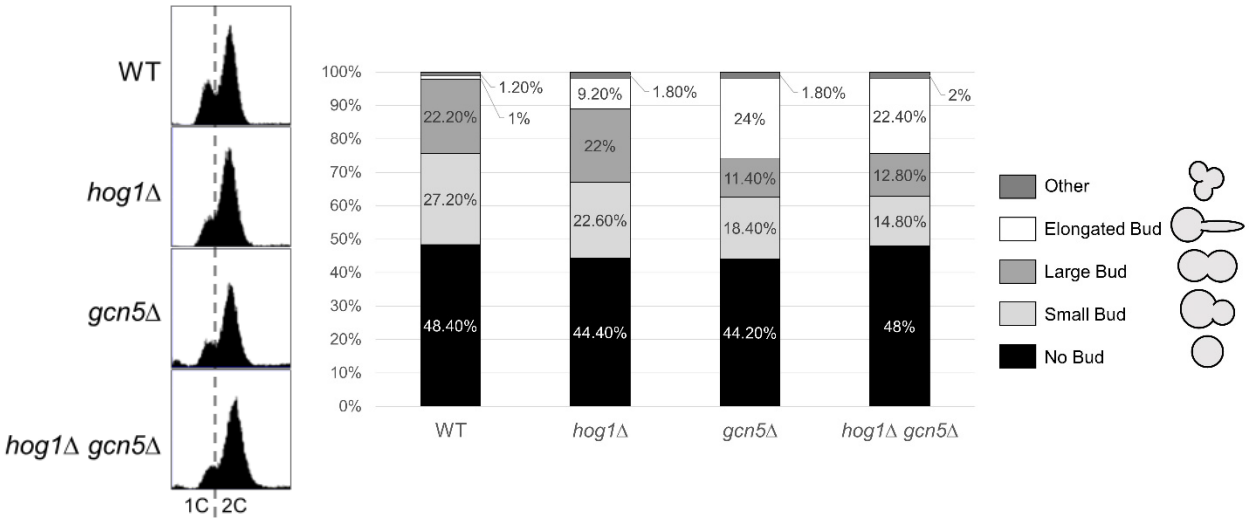

Figure 4C ***hog1*Δ *gcn5*Δ exhibit similar defects as *gcn5*Δ cells.**
Asynchronous WT (LPY 5), *hog1*Δ (LPY 21375), *gcn5*Δ (LPY 13319), *hog1*Δ *gcn5*Δ (LPY 21368) cultures were grown to 0.3 OD, fixed with ethanol. The genetic content is stained with propidium iodide. The processed samples were analyzed with flow cytometry machine by measuring the cell count at certain level of fluorescence emitted by the stained genetic material. 1C indicates 1 copy of the genetic material (G1 phase) while 2C indicate 2 copies of the genetic material (G2/M phase). *hog1*Δ *showed* decreased number of cells in G1 phase, and increased number of cells in S phase. *gcn5*Δ and *hog1*Δ *gcn5*Δ showed similar slow G2/M progression, indicated by an increase in the number of cells in 2C peak and decreased amount of cells in 1C peak. *gcn5*Δ and *hog1*Δ *gcn5*Δ also showed increased number of dead cells compared to WT and *hog1*Δ, indicated by the cell population located on the left corner of the graph.

of cells.

Synchronous *hog1Δ gcn5Δ* culture shows reduced sub-G1 population compared to synchronous *gcn5Δ* culture

We next tested if deletion of *HOG1* improves *gcn5Δ* progression through specific stages of the cell cycle. Mitotic arrest in growing cultures was induced by 1.5-3.75μg/mL nocodazole. After the cells were released from the mitotic arrest (0 mins), samples were collected and stained with propidium iodide for detection of DNA content. In *gcn5Δ* and *hog1Δ gcn5Δ* cultures, accumulation of cells in G1 at 60 mins and a decrease in the G2 population at 90 mins were observed (Figure 4D). In both asynchronous and G2/M synchronized cell cultures, we have found no significant difference in the DNA content and budding index between *gcn5Δ* and *hog1Δ gcn5Δ* (Figure 4C,D). These results indicate that under normal growth conditions in the rich medium, *hog1Δ gcn5Δ* exhibit similar cell cycle defects as *gcn5Δ.* Thus, *hog1Δ* specifically rescues *gcn5Δ* sensitivity to end-point growth on nocodazole, without restoring the cell cycle progression to the WT level.

However, in the flow cytometry analysis, we noticed a significantly lower sub-G1 population in *hog1Δ gcn5Δ* compared to *gcn5Δ* following the nocodazole induced mitotic arrest (Figure 4D). When the percentage of the sub-G1 population at each time point for a single strain is plotted, the median percentages of this population in *gcn5Δ* and *hog1Δ gcn5Δ* are approximately 10% and 6% respectively (Figure 4E). *hog1Δ* greatly decreases the percentage of sub-G1 cells following nocodazole-induced arrest in both WT and *gcn5Δ* backgrounds (Figure 4E). These results suggest that although *hog1Δ* failed to improve *gcn5Δ* cell cycle progression in rich media, *hog1Δ* otherwise

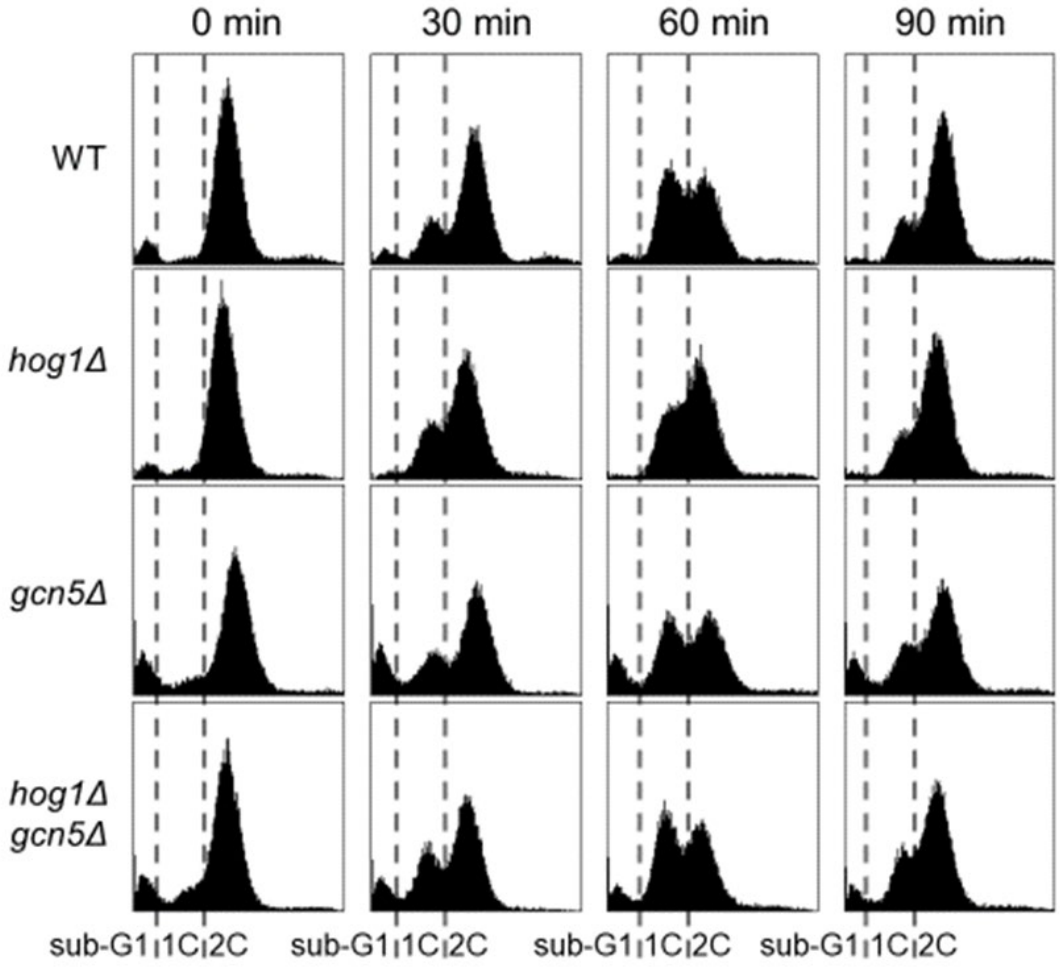

Figure 4D ***hog1*Δ *gcn5*Δ exhibit similar cell cycle progression as *gcn5*Δ cells in nocodazole synchronized cell culture.** Exponentially growing WT (LPY5), hog1Δ (LPY 21375), gcn5Δ (LPY13319), hog1Δ gcn5Δ (LPY 21368) cultures were treated with nocodazole (~3.75ug/ml for WT and hog1Δ, and ~1.5ug/ml for gcn5Δ and hog1Δ gcn5Δ). At T = 0 mins, cultures were released from the arrest, then samples taken every 30 mins and prepared for flow cytometry with total of 30000 events collected. Following nocodazole arrest and release, hog1Δ gcn5Δ shows a decreased sub-G1 population compared to gcn5Δ**.** Those cells with genetic content lower than 1C (fluorescent intensity < 800 AU) are denoted as sub-G1, likely corresponding to apoptotic or significantly aneuploid cells. Whereas cell cycle progression between hog1Δ gcn5Δ and gcn5Δ is similar following nocodazole induced mitotic arrest, a reduction in the Sub-G1 population was observed in hog1Δ gcn5Δ when compared to gcn5Δ.

Figure 4E **Synchronous *hog1Δ gcn5Δ* culture shows reduced sub-G1 population compared to synchronous *gcn5Δ* culture.** Percentage of the sub-G1 population out of the total population detected were quantified and organized into a box. The Sub-G1 population percentages of WT, *hog1Δ, gcn5Δ, hog1Δ gcn5Δ* were shown in blue, orange, grey and yellow, respectively. Single-factor ANOVA was performed separately for WT and *hog1Δ* sub-G1 populations as well as the *gcn5Δ* and *hog1Δ gcn5Δ* (a=0.05). The resulted p-value is reported on the graph. * and ** denotes statistical significance.

alleviates the negative effects caused by nocodazole arrest in *gcn5Δ* mutant. Therefore, we suspected that *hog1Δ* might contribute to increased resistance to nocodazole independently of a direct role in the regulation of cell cycle progression.

hog1Δ Plays a Diverse Role in *gcn5Δ* Cell Cycle Progression

Nocodazole can be used in two different ways in an experiment: to induce cell cycle arrest at the G2/M phase or to monitor the sensitivity of a strain to microtubule destabilization. Previous results showed that the *hog1Δ gcn5Δ* culture contained a decreased sub-G1 population in response to nocodazole-induced G2/M arrest. Based on the results, we hypothesized that *hog1Δ* specifically rescues *gcn5Δ* growth in microtubule destabilizing conditions. Thus, using nocodazole as a microtubule destabilizing agent, we tested if deletion of *HOG1* improves *gcn5Δ* defective cell cycle progression in nocodazole presenting growth conditions. Log-phase cell cultures growing in rich media were treated with nocodazole at 1µg/mL, a lower concentration than that used to induce cell-cycle arrest. The cell cultures were monitored for 6 hours following the addition of nocodazole. In asynchronous cultures growing in 1µg/mL nocodazole, *gcn5Δ* cell cycle progression is disrupted, indicated by an increase in the Sub-G1 and greater than 2C populations (Figure 4F). Deletion of *HOG1* in the *gcn5Δ* mutant resulted in a significant reduction in Sub-G1 and greater than 2C populations, perhaps consistent with a decrease in aneuploidy and apoptotic cells (Figure 4F). Upon nocodazole treatment *hog1Δ gcn5Δ* cultures exhibit an increased 2C population, indicating that cells were accumulating at the G2/M phase (Figure 4F). Furthermore, similar increases in resistance to nocodazole and accumulation at G2/M were also observed in *hog1Δ* when compared to WT at 2µg/mL nocodazole concentration (Figure

4G). These results indicate that loss of Hog1 improves cell cycle progression under microtubule destabilizing conditions.

Deletion of *HOG1* rescues *gcn5Δ hsl1Δ* and *gcn5Δ hsl7Δ* synthetic lethality

Because *hog1*Δ improves *gcn5Δ* cell cycle progression under nocodazole conditions, which hinder but do not halt mitotic progression, we tested if the Hog1-Gcn5 interaction might be further defined in the context of other cell cycle checkpoint functions. Synthetic lethality between *gcn5Δ* and either *hsl1Δ* or *hsl7Δ* was previously characterized (Ruault & Pillus, 2006). This synthetic lethality is rescued by the deletion of *SWE1*, a gene encoding the tyrosine kinase involved in the morphogenesis checkpoint (Ruault & Pillus, 2006). Together these results suggest that constitutive activation of the morphogenesis checkpoint in *gcn5Δ* cells induces synthetic lethality

To test if loss of *HOG1* also rescues this lethality, the triple mutants *hog1Δ gcn5Δ hsl1Δ* and *hog1Δ gcn5Δ hsl7Δ* were constructed, initially supported with a *CEN-URA3-GCN5* plasmid. The mutants were then plated onto 5-FOA to select for the ability to survive in the plasmid's absence. Whereas *gcn5Δ hsl1Δ* and *gcn5Δ hsl7Δ* were inviable on 5-FOA, *hog1Δ gcn5Δ hsl1Δ* and *hog1Δ gcn5Δ hsl7Δ* showed growth comparable to WT strains (Figure 4H). This suppression of *gcn5Δ* synthetic lethality with morphogenesis checkpoint mutants by *hog1Δ* suggests that the Hog1-Gcn5 interaction extends beyond the scope of mitosis and spindle assembly checkpoints. Since both *hog1Δ* and *swe1Δ* rescue *gcn5Δ hsl1Δ* and *gcn5Δ hsl7Δ* synthetic lethality, morphogenesis checkpoint, Hog1 plays a role in inhibiting the cell cycle via checkpoint activation, in the context of nocodazole, deletion of *HOG1* seems to restore normal checkpoint function. Therefore, we conclude that *hog1Δ* plays a diverse and context-

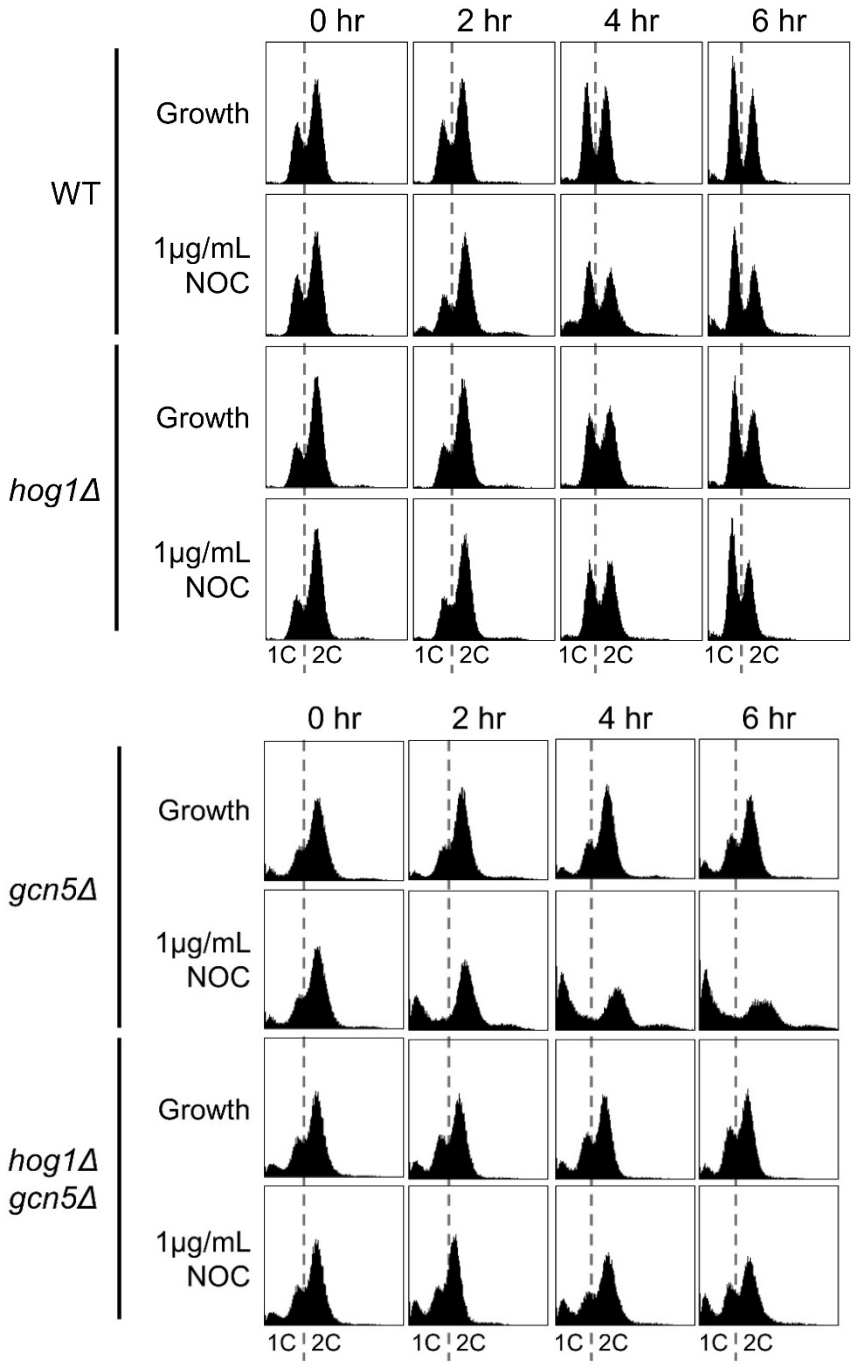

Figure 4F ***hog1Δ* greatly reduces the percentage of sub-G1 and greater-than-2C populations in *gcn5Δ* in liquid YPAD media containing nocodazole**. Exponential cultures of WT (LPY 5), *hog1*Δ (LPY 21375), *gcn5*Δ (LPY 13319), *hog1*Δ *gcn5*Δ (LPY 21368) cells were treated with nocodazole (1 µg/mL) or DMSO (solvent control) and incubated at 30˚C. T= 0 hr denotes the time at which the nocodazole was added cultures and samples were collected and prepared for flow cytometry every hour. WT and *hog1*Δ show a similar pattern of cell cycle progression with marked improvement in cell cycle progression in *hog1*Δ *gcn5*Δ relative to *gcn5*Δ and a decrease

in sub-1C and the greater-than-2C populations in *hog1*Δ *gcn5*Δ*,* indicating a partial relief of aneuploidy.

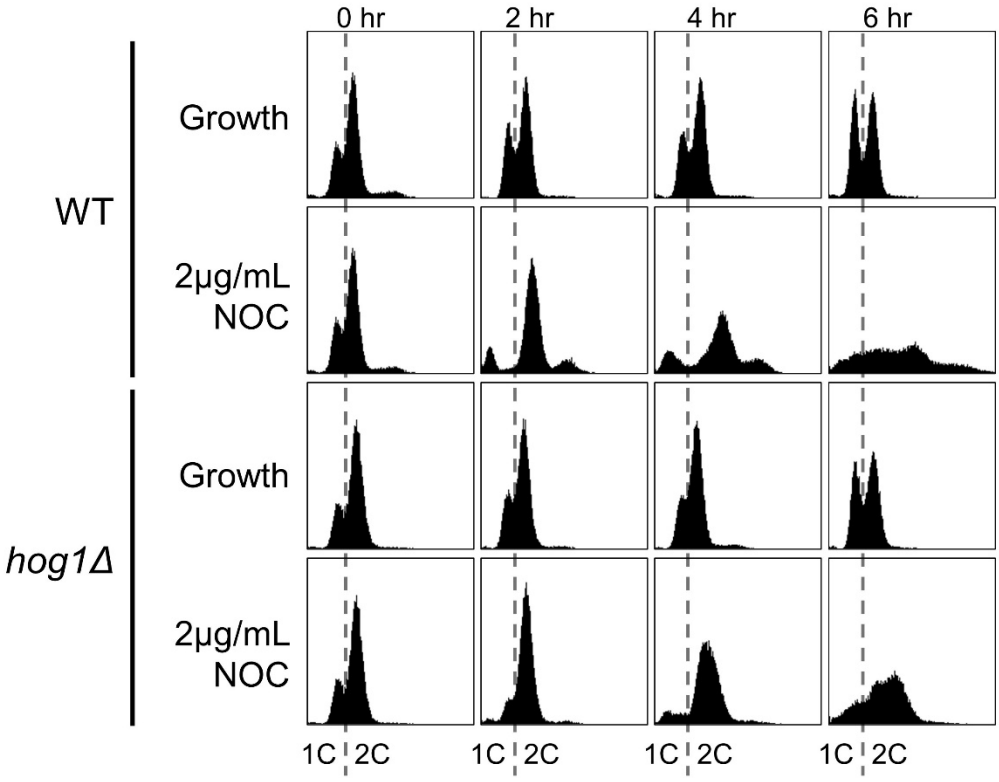

Figure 4G ***hog1Δ* greatly reduces the percentage of sub-G1 and greater-than-2C populations in WT in liquid YPAD media containing nocodazole**
Same method described in figure 4F was used. a drastic improvement in cell cycle progression was observed in *hog1*Δ culture when compared to WT at an elevated nocodazole concentration (2μg/mL)

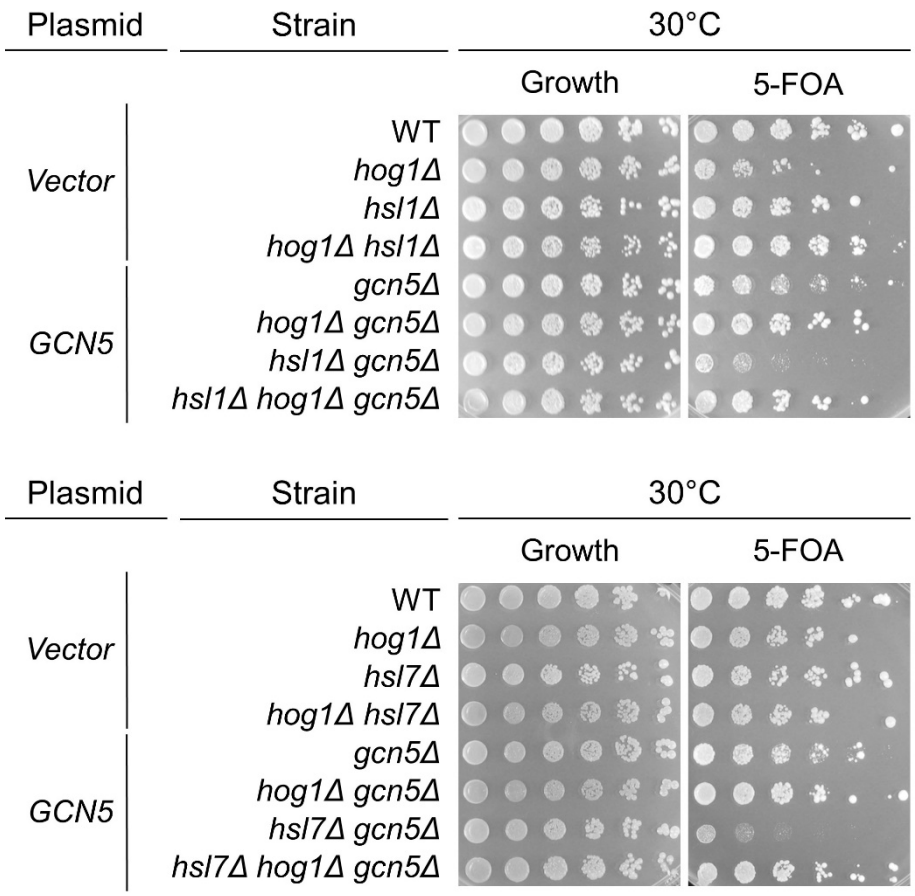

Figure 4H ***hog1*Δ rescues previously reported *gcn5*Δ *hsl1*Δ and *gcn5*Δ *hsl7*Δ synthetic lethality.** Strains were constructed to probe for a role for *HOG1* in the previously observed morphogenesis checkpoint (Rualt and Pillus, 201x) .WT (LPY 5), *hog1Δ* (LPY 21375), *hsl1Δ* (LPY 8937), *hsl7Δ* (LPY 10892), *hog1Δ hsl1Δ, hog1Δ hsl7Δ, gcn5Δ* (LPY 13319), *hog1Δ gcn5Δ* (LPY 21366), *hsl1Δ gcn5Δ* (LPY 9093), *hsl1Δ hog1Δ gcn5Δ, hsl7Δ gcn5Δ* (LPY 10437), *hsl7Δ hog1Δ gcn5Δ* were transformed with pLP 1640 (*CEN-URA3-GCN5*) or pLP 126 (*CEN-URA3-vector*) and plated on URA- (Growth) or 5-FOA. The *gcn5*Δ *hsl1*Δ and *gcn5*Δ *hsl7*Δ were synthetically lethal, whereas *hog1Δ hsl1Δ gcn5Δ* and *hog1Δ hsl7Δ gcn5Δ t*riple mutants survive

dependent role in *gcn5Δ* cell cycle progression.

Discussion

Hog1 Functionally Opposes SAGA and Rts1 Centromeric Function during SAC

During the investigation of the mechanism underlying Hog1-Gcn5 interaction, we found that *hog1Δ* suppresses potential chromosome segregation defects as evidenced by fewer cells with abnormal DNA content in both WT and *gcn5Δ* backgrounds in microtubule destabilizing conditions (Figure 4F, G). Furthermore, *hog1Δ gcn5Δ* cells contain increased G2/M populations under microtubule destabilizing conditions when compared to WT strains (Figure 4G).

During the transition from metaphase to anaphase, proper attachment of spindle fibers to the kinetochore ensures faithful segregation of sister chromatids and prevents aneuploidy and cell death (Li & Murray, 1991). Nocodazole disrupts dynamic microtubule structures leading to activation of the spindle assembly checkpoints during mitosis (Blajeski et al., 2002; Vasquez et al., 1997). Low nocodazole concentrations mainly affect the spindle fiber interaction with kinetochore without major structural changes to the spindle fibers (Y. Wang & Burke, 1995). Therefore, we propose that under microtubule destabilizing conditions induced by the low dose 1μg/mL nocodazole treatment, deletion of *HOG1* slows the kinetics of cell cycle progression, allowing for proper kinetochore-microtubule attachments to stabilize under otherwise less-than-ideal conditions. Accordingly, lower numbers of apoptotic and aneuploid cells were observed. The increased G2/M population in *hog1Δ gcn5Δ* further supports this interpretation.

Reiser et al 2006 reported that sustained activation of the HOG pathway rescues the mitotic exit defects in MEN. The results reported here bear resemblance to these

observations in that no distinct improvement was observed in *hog1Δ gcn5Δ* cell cycle progression when compared to *gcn5Δ* under normal growth conditions. However, improvement in cell cycle progression was observed when nocodazole was introduced to growth media, akin to inhibiting mitotic exit. Furthermore, *hog1Δ* mutants showed a significant delay in the spindle disassembly checkpoint under normal growth conditions (Pigula et al., 2014). Together, these results imply that in the context of mitosis, Hog1 may have a role in promoting mitotic progression and exit, acting in opposition to checkpoints that halt cell cycle progression. Based on our results and previous studies, we suspected that this specific function of Hog1 might be independent of the cell cycle modulation mediated by Hog1 upon osmotic shock. Indeed, Hog1 was found to delay mitotic exit by facilitating anaphase onset during osmotic stress (Tognetti, Jiménez et al., 2020).

Previous studies have shown that Gcn5 plays an important role in the centromeric localization of Rts1, which in turn promotes the tension sensing function of the spindle assembly checkpoint (Petty et al., 2018). We hypothesize that Hog1 functionally opposes the Gcn5 and Rts1-mediated checkpoint. Upon microtubule destabilization, Hog1 may be activated to promote mitotic exit and oppose the cell cycle arrest induced by the SAC mediated by Gcn5 and $PP2A^{Rts1}$(Figure 4I). In WT cells, a balance between the effects imposed on the cell cycle by Gcn5/Rts1 and Hog1 ensures the cells undergo faithful chromosome segregation without prolonged mitotic stalling or arrest. However, in *gcn5Δ* mutants where the checkpoint is defective, Hog1-related induction of mitotic exit could exacerbate the defective checkpoint (Figure 4I). Thus,

deletion of *HOG1* alleviates the chromosome segregation defect in *gcn5Δ* cells and increases the overall G2/M population when treated with nocodazole.

Previous studies demonstrated that a balance of dynamic phosphorylation at the centromere has a profound consequence on the interaction between the kinetochore and spindle fibers (Liu et al., 2010). One possibility is that Hog1directly opposes SAC and promotes mitotic exit by phosphorylating the centromeric-specific histone protein Cse4. A single threonine residue, Cse4-T133, aligns with the phosphorylation consensus site of Hog1. Hog1 and $PP2A^{Rts1}$ thus potentially mediate a balance of phosphorylation at the centromere, modulating the spindle assembly checkpoint. Additionally, Hog1 might indirectly promote mitotic exit via interaction with cell cycle checkpoint components since Hog1 has been shown to mediate cell cycle arrest via modulation of cyclin expression and CDK inhibition under osmotic stress (Escoté, Zapater, Clotet et al., 2004, Yaakov et al., 2009, Clotet, Escoté, Adrover et al., 2006, Tognetti, Jiménez et al., 2020). Other studies have also shown that Hog1 recruits the histone deacetylase Rpd3 to osmotic stress gene promoters to modulate the transcription of stress-responsive genes (De Nadal et al., 2004). Therefore, loss of Hog1 in *gcn5Δ* cells might restore the acetylation balance on key histone residues, thus improving *gcn5Δ* cell cycle progression.

The Many Faces of *hog1Δ* in *gcn5Δ* Cell Cycle Progression

Beyond defective mitotic progression in *gcn5Δ* mutants, as evident by *gcn5Δ* sensitivity to the overexpression of Clb2 (Krebs et al., 2000), *gcn5Δ* disturbs other stages of cell cycle progression, including a significant reduction in the centromeric localization of Rts1 during the spindle assembly checkpoint, and slower progression of

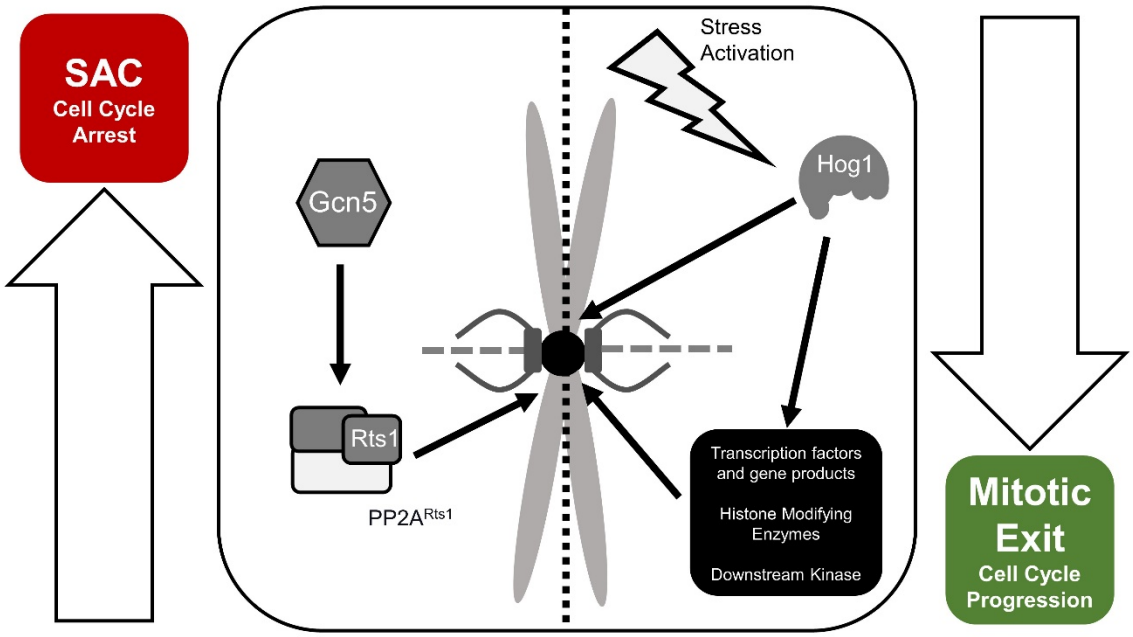

Figure 4I **Gcn5/Rts1 and Hog1 function respectively in arresting and driving cell cycle progression during spindle assembly checkpoint.**
Previously, we have identified that Gcn5-containing SAGA promotes Rts1 localization to centromeres, which is crucial for the activation of the spindle assembly checkpoint (SAC) We propose that under microtubule destabilizing conditions, Gcn5 acts within SAGA to promote Rts1 localization to the centromere, which result in SAC activation and cell cycle arrest. At the same time, Hog1, activated via an unknown stress, promotes mitotic exit via either direct interaction with the centromere or indirect mechanisms involving other players. We propose that under microtubule destabilizing conditions, Hog1 functionally opposes Rts1 and Gcn5. A balance between Gcn5/Rts1 mediated SAC and Hog1 promoted mitotic exit ensures faithful segregation of chromosome.

G1/S and G2/M (Petty et al., 2016, 2018). Based on the results from this study, we propose that Hog1 might play different roles in *gcn5Δ* cell cycle progression based on the specific interaction partner and the context of the interaction. Whereas we hypothesize that Hog1 plays a role in promoting mitotic exit in its interaction with Gcn5 and Rts1 in the context of spindle assembly checkpoint, *hog1Δ* suppression of *gcn5Δ* synthetic lethality with morphogenesis checkpoint mutants suggests that in the context of the morphogenesis checkpoint, Hog1 plays a role in promoting cell cycle arrest. During the G2/M transition, timely Swe1 degradation depends on Hsl1 and Hsl7 and promotes the progression of the cell cycle. Loss of either Hsl1 or Hsl7 resulted in a constitutively activated morphogenesis checkpoint (McMillan et al., 1999). Previous studies identified the deletion of *SWE1,* a gene encoding a CDK inhibitor that regulates G2/M progression, as a suppressor of *gcn5Δ* lethality under a constitutively activated morphogenesis checkpoint (Ruault & Pillus, 2006). Deletion of either *HOG1* or *SWE1* rescues *gcn5Δ hsl1Δ* and *gcn5Δ hsl7Δ* synthetic lethality, indicating that in the context of the morphogenesis checkpoint in *gcn5Δ*, Hog1 and Swe1 play similar roles in the negative regulation of cell cycle progression. Indeed, upon sensing osmotic stress, Hog1 was found to phosphorylate Hsl1, promoting Swe1 stabilization and G2/M arrest (Clotet, Escoté, Adrover et al., 2006). Together, these results suggest that there are multiple aspects of the Hog1-Gcn5 functional interaction contributing to cell cycle progression. The stage of the cell cycle, as well as the interacting partners, determine the role played by Hog1 and Gcn5 respectively.

In conclusion, through genetic analysis, we identified a previously unknown Hog1-Rts1-Gcn5 interaction in the context of histone modification and cell cycle

progression. Our data support a hypothesis in which Hog1 and Rts1/Gcn5 functionally oppose each other at the spindle assembly checkpoint, pointing to a new function of the HOG pathway in the context of cell cycle checkpoint functions beyond response to hyperosmolarity stress.

Chapter 4, in part is currently being prepared for submission for publication of the material. Liu, Qihao; Petty, Emily; Pillus, Lorraine. The thesis author was the primary investigator and author of this material.

APPENDIX 1 MATERIALS AND METHODS

Yeast methods

Standard protocols for yeast growth were used (Guthrie & Fink, 1991). All yeast strains were grown at 30°C, except where indicated. For dilution assays, yeast cultures were adjusted to 1.0 OD_{600}/ml and further diluted in 5-fold increments. Plates were photographed after 2 to 5 days of incubation, as indicated in the figure legends. To test the effects of specific histone mutations, histone shuffle strains were constructed, with the WT histone shuffle strain (LPY 14461 *hht1-hhf1*Δ::*kanMX hta1-htb1*Δ::*natMX hta2-htb2*Δ::*HPH*) crossed to *hog1*Δ *gcn5*Δ (LPY 21366) to produce the *hog1*Δ *hht1-hhf1*Δ::*kanMX hta1-htb1*Δ::*natMX hta2-htb2*Δ::*HPH (*LPY 23129*)* and the *hog1*Δ *gcn5*Δ *hht1-hhf1*Δ::*kanMX hta1-htb1*Δ::*natMX hta2-htb2*Δ::*HPH* (LPY 23127) strains. Mutant *htb1* plasmids (*htb1-T94A, htb1-T91E, or htb1-T91D*) were transformed into the histone shuffle strains containing a *URA3*-WT histone plasmid. The strains used are listed in Table S.1. Yeast transformations were performed with either simple colony-based or lithium acetate-based protocols. The plasmids used are listed in Table S.2.

Cells analyzed for the budding index were taken from log-phase cultures and fixed with 70% cold ethanol. Unbudded cells, those with small buds, and large buds roughly correspond to those in the population undergoing the G1, S, and G2/M phases of the cell cycle. Cells with elongated buds and other abnormal budding patterns likely result from disruption of the budding cycle or other manifestations of mutants.

Media preparation

Yeast media were prepared with standard protocols, with modifications as noted (Guthrie and Fink, 1991; Sherman et al., 1991). Hydroxyurea (HU) plates were prepared by adding filter-sterilized 1M HU stock solution to synthetic complete (SC) or YPAD (Yeast extract Peptone Adenine Dextrose) media to a final concentration of 0.1M or 0.05M. Methyl methanesulfonate (MMS) plates were prepared at final concentrations of 0.01% to 0.025% in SC or YPAD. Camptothecin (CPT) was added from a 3 mg/mL stock dissolved in DMSO to YPAD media buffered to pH 7.5 by potassium phosphate buffer to a final concentration of 3μg/mL to 12μg/mL. DMSO plates were prepared as solvent control. Nocodazole (NOC) plates were prepared by adding 10mg/ml of nocodazole dissolved in DMSO to YPAD to a final concentration of 1μg/mL to 2μg/mL. KCl and Sorbitol plates were prepared by adding filter-sterilized KCl and Sorbitol solution to YPAD media to a final concentration of 1M KCl or 1M Sorbitol. 5-FOA plates were prepared by adding filter-sterilized 5-FOA solution to SC media to a final concentration of 0.5X (~0.0057M). 0.5x 5-FOA concentration is used due to increased sensitivity in the *gcn5Δ* background.

Bacterial transformation

100ul of the calcium-competent DH5α *E.Coli* cells were mixed with 5-10ul of DNA and incubated on ice for 30mins to 1hr. Competent cells were heat-shocked at 42°C for 45s before recovering on ice for 1-2mins. The cells were incubated in 1ml fresh LB at 37°C for 45mins to 1hr before plating on the selective media plate

Simple transformation of yeast

Yeast transformation is performed by mixing 1ug of minipreped plasmid DNA, 10ul of 10mg/ml ssDNA, and 0.5ml PLATE (PEG-4000, Lithium Acetate, Tris-HCl pH 7.5, EDTA) solution. Transformation mixes were incubated at room temperature for four hours to overnights. Post-incubation, the cell pellets are resuspended in 1M sorbitol or yeast nitrogenous base solution and plated onto the corresponding auxotrophic plates. Plasmids used in this study were listed in table S.2.

Lithium acetate transformation of yeast

WT yeast cells were made competent with 1X TEL at room temperature overnight. 10uL ssDNA and 1ug of DNA were mixed with 100ul of competent yeast cells. 700 ul of 40% PEG-4000 in TEL buffer was added to the mixture. The transformants were incubated at room temperature for 30mins and heat shock at 42 °C for 15mins. The spun-down cell pellets were resuspended in yeast nitrogenous base media and plated onto selective media.

5-FOA Counterselection

5-FOA plates were prepared by adding filter-sterilized 5-FOA solution to SC media to a final concentration of 0.5X (~0.0057M). 0.5x 5-FOA concentration is used due to increased sensitivity in the *gcn5Δ* background. Transformants containing *URA3* plasmid were plated onto 5-FOA plates to select for loss of the *URA3* plasmid. In the synthetic lethality test, a *URA3* plasmid carrying the *WT-GCN5* gene is transformed into

the combinational mutant. The transformants were plated onto 5-FOA to select for mutants that do not require a copy of *WT-GCN5* to grow.

Flow cytometry

Samples were taken from exponentially growing cell cultures and fixed with cold 70% ethanol at 4°C overnight. Following fixation, the samples were treated with RNAse A (will add concentration) at 37 °C overnight and stained with propidium iodide (PI) at 4°C overnight. All experiments used a BD ACURI C6 flow cytometer for analysis. Fluorescence was collected with the FL2A channel with fluidics were set to slow with an event limit of 30,000 events. During measurement, collected data were visualized in the BD ACURI C6 flow cytometer histogram software. Microsoft Excel was used for statistical analysis and presentation.

Nocodazole sensitivity assay

10mg/ml nocodazole dissolved in DMSO was added to log-phase cultures for a final concentration of 1μg/mL to 2μg/mL. Samples were collected every hour for 6 to 8 hours following the nocodazole treatment. The samples collected were analyzed with flow cytometry as described above.

CRISPR mutagenesis

The *hog1-T174A* catalytic mutation was introduced via CRISPR-mediated mutagenesis in a protocol adapted from McDonnell *et al*. (2000). CRISPR Direct (https://crispr.dbcls.jp/) was used for the identification of PAM sequence and guide RNA

location within the *HOG1* sequence. The plasmid pML104, which encodes the Cas9 protein (a gift from L. McDonnell, UCSD), was digested with BclI and SwaI. Oligos containing a BclI 5' overhang, *HOG1* gRNA sequence, and Cas9 scaffold sequence were hybridized and subsequently ligated into pML104. The homology directed repair template was synthesized via PCR with a pair of overlapping primers containing the *hog1-T174A* mutation and the PAM disrupting silent mutation. The PAM (NGG) sequence was disrupted with a silent mutation, and the newly introduced codon at the PAM site and on threonine 174 were confirmed to be one of the preferred codons for yeast. The constructed CRISPR plasmid and the HDR templates were transformed into yeast cells via the lithium acetate method. *hog1-T174A* cells were selected based on positive growth on URA– media and a lack of growth on 1M sorbitol media. The genotype was confirmed by sequencing PCR amplified products from genomic DNA (adapted from Hoffman & Winston, 1987). Oligo nucleotides used for CRISPR mutagenesis are presented in Table S3.

Table S.1 Strains used in this study. All strains were constructed in this study or obtained from the lab collection.

Strain	Genotype
LPY 5	*MATa ade2-1 can1-100 his3-11 leu2-3,112 trp1-1 ura3-1 GAL*
LPY 1873	*MATa ade2-1 can1-100 his3-11 leu2-3,112 trp1-1 ura3-1 GAL kss1Δ::KanMX*
LPY 8156	*MATa ade2-1 can1-100 his3-11 leu2-3,112 trp1-1 ura3-1 GAL snf1Δ::KanMX*
LPY 8653	*MATa ade2-1 can1-100 his3-11 leu2-3,112 trp1-1 ura3-1 GAL swe1Δ::KanMX gcn5Δ::NatMX*
LPY 8937	*MATa ade2-1 can1-100 his3-11 leu2-3,112 trp1-1 ura3-1 GAL hsl1Δ::KanMX*
LPY 8939	*MATa ade2-1 can1-100 his3-11 leu2-3,112 trp1-1 ura3-1 GAL gcn5Δ::NatMX*
LPY 9093	*MATa ade2-1 can1-100 his3-11 leu2-3,112 trp1-1 ura3-1 GAL hsl1Δ::KanMX gcn5Δ::NatMX*
LPY 9400	*MATa ade2-1 can1-100 his3-11 leu2-3,112 trp1-1 ura3-1 GAL swe1Δ::KanMX*
LPY 9573	*MATa ade2-1 can1-100 his3-11 leu2-3,112 trp1-1 ura3-1 GAL hsl7Δ::HIS3*
LPY 10892	*MATa ade2-1 can1-100 his3-11 leu2-3,112 trp1-1 ura3-1 GAL hsl7Δ::HIS3 gcn5Δ::NatMX*
LPY 13319	*MATa ade2-1 can1-100 his3-11 leu2-3,112 trp1-1 ura3-1 GAL gcn5Δ::NatMX*
LPY 13440	*MATa ade2-1 can1-100 his3-11 leu2-3,112 trp1-1 ura3-1 GAL snf1Δ::KanMX gcn5Δ::NatMX*
LPY 14462	*MATa ade2-1 can1-100 his3-11 leu2-3,112 trp1-1 ura3-1 GAL hht1-hhf1Δ::KanMX hta1-htb1Δ::NatMX hta2-htb2Δ::HPH*
LPY 15179	*MATa ade2-1 can1-100 his3-11 leu2-3,112 trp1-1 ura3-1 GAL rts1Δ::KanMX gcn5Δ::NatMX*
LPY 16356	*MATa ade2-1 can1-100 his3-11 leu2-3,112 trp1-1 ura3-1 GAL sch9Δ::KanMX*
LPY 16434	*MATa ade2-1 can1-100 his3-11 leu2-3,112 trp1-1 ura3-1 GAL hht1-hhf1Δ::KanMX hta1-htb1Δ::NatMX hta2-htb2Δ::HPH gcn5Δ::NatMX*
LPY 16960	*MATa ade2-1 can1-100 his3-11 leu2-3,112 trp1-1 ura3-1 GAL*
LPY 17138	*MATa ade2-1 can1-100 his3-11 leu2-3,112 trp1-1 ura3-1 GAL sch9Δ::KanMX gcn5Δ::NatMX*
LPY 18171	*MATa ade2-1 can1-100 his3-11 leu2-3,112 trp1-1 ura3-1 GAL kss1Δ::KanMX gcn5Δ::NatMX*
LPY 18426	*MATa ade2-1 can1-100 his3-11 leu2-3,112 trp1-1 ura3-1 GAL cla4Δ::KanMX*
LPY 18427	*MATa ade2-1 can1-100 his3-11 leu2-3,112 trp1-1 ura3-1 GAL pho85Δ::KanMX*
LPY 18491	*MATa ade2-1 can1-100 his3-11 leu2-3,112 trp1-1 ura3-1 GAL pho85Δ::KanMX gcn5Δ::NatMX*
LPY 19608	*MATa ade2-1 can1-100 his3-11 leu2-3,112 trp1-1 ura3-1 GAL slt2Δ::KanMX gcn5Δ::NatMX*

Table S.1 Strains used in this study. All strains were constructed in this study or obtained from the lab collection. (Continued)

Strain	Genotype
LPY 19785	*MATa ade2-1 can1-100 his3-11 leu2-3,112 trp1-1 ura3-1 GAL tel1Δ::KanMX*
LPY 20086	*MATa ade2-1 can1-100 his3-11 leu2-3,112 trp1-1 ura3-1 GAL chk1Δ:;KanMX*
LPY 20132	*MATa ade2-1 can1-100 his3-11 leu2-3,112 trp1-1 ura3-1 GAL tel1Δ::KanMX gcn5Δ::NatMX*
LPY 20224	*MATa ade2-1 can1-100 his3-11 leu2-3,112 trp1-1 ura3-1 GAL ctk1Δ::KanMX*
LPY 20227	*MATa ade2-1 can1-100 his3-11 leu2-3,112 trp1-1 ura3-1 GAL dun1Δ::KanMX*
LPY 20298	*MATa ade2-1 can1-100 his3-11 leu2-3,112 trp1-1 ura3-1 GAL chk1Δ::KanMX gcn5Δ::NatMX*
LPY 20366	*MATa ade2-1 can1-100 his3-11 leu2-3,112 trp1-1 ura3-1 GAL ctk1Δ::KanMX gcn5Δ::NatMX*
LPY 20370	*MATa ade2-1 can1-100 his3-11 leu2-3,112 trp1-1 ura3-1 GAL dun1Δ::KanMX gcn5Δ::NatMX*
LPY 20612	*MATa ade2-1 can1-100 his3-11 leu2-3,112 trp1-1 ura3-1 GAL (HA)3-(HIS)6-cse4-S135A*
LPY 20668	*MATa ade2-1 can1-100 his3-11 leu2-3,112 trp1-1 ura3-1 GAL gcn5Δ::NatMX (HA)3-(HIS)6-cse4-S135A*
LPY 20780	*MATa ade2-1 can1-100 his3-11 leu2-3,112 trp1-1 ura3-1 GAL gcn5Δ::NatMX (HA)3-(HIS)6-cse4-S180A*
LPY 20786	*MATa ade2-1 can1-100 his3-11 leu2-3,112 trp1-1 ura3-1 GAL (HA)3-(HIS)6-CSE4*
LPY 20788	*MATa ade2-1 can1-100 his3-11 leu2-3,112 trp1-1 ura3-1 GAL gcn5Δ::NatMX (HA)3-(HIS)6-CSE4*
LPY 20827	*MATa ade2-1 can1-100 his3-11 leu2-3,112 trp1-1 ura3-1 GAL (HA)3-(HIS)6-cse4-S180A*
LPY 21070	*MATa ade2-1 can1-100 his3-11 leu2-3,112 trp1-1 ura3-1 GAL rad53Δ::KanMX*
LPY 21366	*MATa ade2-1 can1-100 his3-11 leu2-3,112 trp1-1 ura3-1 GAL hog1Δ:: KanMX gcn5Δ:: NatMX*
LPY 21374	*MATa ade2-1 can1-100 his3-11 leu2-3,112 trp1-1 ura3-1 GAL hog1Δ::KanMX*
LPY 21388	*MATa ade2-1 can1-100 his3-11 leu2-3,112 trp1-1 ura3-1 GAL rad53Δ::KanMX gcn5Δ::NatMX*
LPY 21648	*MATa ade2-1 can1-100 his3-11 leu2-3,112 trp1-1 ura3-1 GAL cka1Δ::KanMX*
LPY 21650	*MATa ade2-1 can1-100 his3-11 leu2-3,112 trp1-1 ura3-1 GAL cka2Δ::KanMX*
LPY 21669	*MATa ade2-1 can1-100 his3-11 leu2-3,112 trp1-1 ura3-1 GAL cka1Δ::KanMX gcn5Δ::NatMX*
LPY 21673	*MATa ade2-1 can1-100 his3-11 leu2-3,112 trp1-1 ura3-1 GAL cka2Δ::KanMX gcn5Δ::NatMX*
LPY 23002	*MATa ade2-1 can1-100 his3-11 leu2-3,112 trp1-1 ura3-1 GAL cla4Δ::KanMX gcn5Δ::NatMX*

Table S.1 Strains used in this study. All strains were constructed in this study or obtained from the lab collection. (Continued)

Strain	Genotype
LPY 23013	*MATa ade2-1 can1-100 his3-11 leu2-3,112 trp1-1 ura3-1 GAL slt2Δ::KanMX*
LPY 23127	*MATa ade2-1 can1-100 his3-11 leu2-3,112 trp1-1 ura3-1 GAL hht1-hhf1Δ::KanMX hta1-htb1Δ::NatMX hta2-htb2Δ::HPH hog1Δ::KanMX gcn5Δ::NatMX*
LPY 23129	*MATa ade2-1 can1-100 his3-11 leu2-3,112 trp1-1 ura3-1 GAL hht1-hhf1Δ::KanMX hta1-htb1Δ::NatMX hta2-htb2Δ::HPH gcn5Δ::NatMX*
LPY 23135	*MATa ade2-1 can1-100 his3-11 leu2-3,112 trp1-1 ura3-1 GAL hog1Δ::KanMX gcn5Δ::NatMX (HA)3-(HIS)6-cse4-S180A*
LPY 23136	*MATa ade2-1 can1-100 his3-11 leu2-3,112 trp1-1 ura3-1 GAL hog1Δ::KanMX gcn5Δ::NatMX (HA)3-(HIS)6-CSE4*
LPY 23137	*MATa ade2-1 can1-100 his3-11 leu2-3,112 trp1-1 ura3-1 GAL hog1Δ::KanMX gcn5Δ::NatMX (HA)3-(HIS)6-cse4-S135A*
LPY 23138	*MATa ade2-1 can1-100 his3-11 leu2-3,112 trp1-1 ura3-1 GAL hog1Δ::KanMX (HA)3-(HIS)6-cse4-S180A*
LPY 23139	*MATa ade2-1 can1-100 his3-11 leu2-3,112 trp1-1 ura3-1 GAL hog1Δ::KanMX (HA)3-(HIS)6-CSE4*
LPY 23140	*MATa ade2-1 can1-100 his3-11 leu2-3,112 trp1-1 ura3-1 GAL hog1Δ::KanMX (HA)3-(HIS)6-cse4-S135A*
LPY 23147	*MATa ade2-1 can1-100 his3-11 leu2-3,112 trp1-1 ura3-1 GAL hog1-T174A*
LPY 23150	*MATa ade2-1 can1-100 his3-11 leu2-3,112 trp1-1 ura3-1 GAL hog1-T174A gcn5Δ::NatMX*
LPY 23189	*MATa ade2-1 can1-100 his3-11 leu2-3,112 trp1-1 ura3-1 GAL hog1Δ::KanMX gcn5Δ::NatMX rts1Δ::KanMX*
LPY 23190	*MATa ade2-1 can1-100 his3-11 leu2-3,112 trp1-1 ura3-1 GAL hog1-T174A gcn5Δ::NatMX rts1Δ::KanMX*
LPY 23191	*MATa ade2-1 can1-100 his3-11 leu2-3,112 trp1-1 ura3-1 GAL hog1Δ::KanMX hsl1Δ::KanMX*
LPY 23192	*MATa ade2-1 can1-100 his3-11 leu2-3,112 trp1-1 ura3-1 GAL hsl1Δ::KanMX hog1Δ::KanMX gcn5Δ::NatMX*
LPY 23193	*MATa ade2-1 can1-100 his3-11 leu2-3,112 trp1-1 ura3-1 GAL hsl7Δ::HIS3 hog1Δ::KanMX gcn5Δ::NatMX*
LPY 23194	*MATa ade2-1 can1-100 his3-11 leu2-3,112 trp1-1 ura3-1 GAL hog1Δ::KanMX hsl7Δ::HIS3*

Table S.2 Plasmids included in the study. Unless otherwise noted, plasmids were constructed in this study or obtained from the lab collection.

Plasmid	Genotype	Source
pLP 60	*CEN-HIS3-Vector*	
pLP 126	*CEN-URA3-Vector*	
pLP 1640	*CEN-URA3-GCN5*	
pLP 2212	*CEN-URA3-HTA1-HTB1-HHT1-HHF1*	M.M. Smith
pLP 2482	*CEN-HIS3-HTA1-htb1-T91A-FLAG*	
pLP 2492	*CEN-HIS3-HTA1-HTB1-FLAG*	
pLP 2689	*CEN-HIS3-HTA1-htb1-T91E-FLAG*	
pLP 2770	*CEN-HIS3-HTA1-htb1-T91D-FLAG*	
pLP 3508	*CEN-URA3-CAS9*	L. McDonnell
pLP 3512	*CEN-HIS3-HOG1*	
pLP 3513	*CEN-HIS3-hog1-T174A*	

Table S.3 Oligonucleotides included in the study.

Oligo	Gene	Use	Sequence
oLP 2362	*HOG1*	Cloning	GGTAGCCCTTCATTACGGCATAACG
oLP 2363	*HOG1*	Cloning and Sequencing	CCTTTTTCTTCCAGTTTTACTAGTAAATCCAATGCGG
oLP 2491	*HOG1*	Sequencing	GCTCAGCCACGGACACTTTG
oLP 2506	*HOG1*	Mutagenesis	GAATTCAAGACCCTCAAATGGCAGGCTATGTTTCCAC
oLP 2507	*HOG1*	Mutagenesis	GTGGAAACATAGCCTGCCATTTGAGGGTCTTGAATTC
oLP 2508	*HOG1*	gRNA	/5Phos/GATCAGGTGCCCTGTAGTATCTAGGTTTTAGAGCTAG
oLP 2509	*HOG1*	gRNA	/5Phos/CTAGCTCTAAAACCTAGATACTACAGGGCACCT
oLP 2510	*HOG1*	HDR	CGGTCTAGCAAGAATTCAAGACCCTCAAATGGCAGGCTATGTTTCTACTAGATACTACAG
oLP 2511	*HOG1*	HDR	CGTCATATTTTTGCCACGTTAGCATGATTTCAGGTGCCCTGTAGTATCTAGTAGAAAC

BIBLIOGRAPHY

Ahn, S. H., Cheung, W. L., Hsu, J. Y., Diaz, R. L., Smith, M. M., & Allis, C. D. (2005). Sterile 20 kinase phosphorylates histone H2B at serine 10 during hydrogen peroxide-induced apoptosis in *S. cerevisiae*. Cell, 120(1), 25–36. https://doi.org/10.1016/j.cell.2004.11.016

Alvino, G. M., Collingwood, D., Murphy, J. M., Delrow, J., Brewer, B. J., & Raghuraman, M. K. (2007). Replication in Hydroxyurea: It's a Matter of Time. Molecular and Cellular Biology, 27(18), 6396–6406. https://doi.org/10.1128/mcb.00719-07

Ardito, F., Giuliani, M., Perrone, D., Troiano, G., & Muzio, L. Lo. (2017). The crucial role of protein phosphorylation in cell signalingand its use as targeted therapy (Review). International Journal of Molecular Medicine, 40(2), 271–280. https://doi.org/10.3892/ijmm.2017.3036

Asano, S., Park, J. E., Sakchaisri, K., Yu, L. R., Song, S., Supavilai, P., Veenstra, T. D., & Lee, K. S. (2005). Concerted mechanism of Swe1/Wee1 regulation by multiple kinases in budding yeast. EMBO Journal, 24(12), 2194–2204. https://doi.org/10.1038/sj.emboj.7600683

Baker, S. P., & Grant, P. A. (2007). The SAGA continues: Expanding the cellular role of a transcriptional co-activator complex. Oncogene, 26(37), 5329–5340. https://doi.org/10.1038/sj.onc.1210603

Bannister, A. J., & Kouzarides, T. (2011). Regulation of chromatin by histone modifications. Cell Research, 21(3), 381–395. https://doi.org/10.1038/cr.2011.22

Barnes, C. E., English, D. M., & Cowley, S. M. (2019). Acetylation and Co: An expanding repertoire of histone acylations regulates chromatin and transcription. Essays in Biochemistry, 63(1), 97–107. https://doi.org/10.1042/EBC20180061

Barral, Y., Parra, M., Bidlingmaier, S., & Snyder, M. (1999). Nim1-related kinases coordinate cell cycle progression with the organization of the peripheral cytoskeleton in yeast. Genes and Development, 13(2), 176–187. https://doi.org/10.1101/gad.13.2.176

Blajeski, A. L., Phan, V. A., Kottke, T. J., & Kaufmann, S. H. (2002). G1 and G2 cell-cycle arrest following microtubule depolymerization in human breast cancer cells. Journal of Clinical Investigation, 110(1), 91–99. https://doi.org/10.1172/JCI13275

Boeke, J. D., Trueheart, J., Natsoulis, G., & Fink, G. R. (1987). [10] 5-Fluoroorotic acid as a selective agent in yeast molecular genetics. Methods in Enzymology, 154(C), 164–175. https://doi.org/10.1016/0076-6879(87)54076-9

Boutros, M., & Ahringer, J. (2008). The art and design of genetic screens: RNA interference. Nature Reviews Genetics, 9(7), 554–566. https://doi.org/10.1038/nrg2364

Brewster, J. L., & Gustin, M. C. (2014). Hog1: 20 years of discovery and impact. Science Signaling, 7(343), 1–11. https://doi.org/10.1126/scisignal.2005458

Bu, P., Evrard, Y. A., Lozano, G., & Dent, S. Y. R. (2007). Loss of Gcn5 Acetyltransferase Activity Leads to Neural Tube Closure Defects and Exencephaly in Mouse Embryos. Molecular and Cellular Biology, 27(9), 3405–3416. https://doi.org/10.1128/mcb.00066-07

Burgess, R. J., & Zhang, Z. (2010). Histones, histone chaperones and nucleosome assembly. Protein and Cell, 1(7), 607–612. https://doi.org/10.1007/s13238-010-0086-y

Campbell, I. W., Zhou, X., & Amon, A. (2019). The mitotic exit network integrates temporal and spatial signals by distributing regulation across multiple components. ELife, 8, 1–23. https://doi.org/10.7554/eLife.41139

Carré, C., Szymczak, D., Pidoux, J., & Antoniewski, C. (2005). The Histone H3 Acetylase dGcn5 Is a Key Player in Drosophila melanogaster Metamorphosis . Molecular and Cellular Biology, 25(18), 8228–8238. https://doi.org/10.1128/mcb.25.18.8228-8238.2005

Castermans, D., Somers, I., Kriel, J., Louwet, W., Wera, S., Versele, M., Janssens, V., & Thevelein, J. M. (2012). Glucose-induced posttranslational activation of protein phosphatases PP2A and PP1 in yeast. Cell Research, 22(6), 1058–1077. https://doi.org/10.1038/cr.2012.20

Caydasi, A. K., Ibrahim, B., & Pereira, G. (2010). Monitoring spindle orientation: Spindle position checkpoint in charge. Cell Division, 5, 1–15. https://doi.org/10.1186/1747-1028-5-28

Cherry, J. M., Hong, E. L., Amundsen, C., Balakrishnan, R., Binkley, G., Chan, E. T., Christie, K. R., Costanzo, M. C., Dwight, S. S., Engel, S. R., Fisk, D. G., Hirschman, J. E., Hitz, B. C., Karra, K., Krieger, C. J., Miyasato, S. R., Nash, R. S., Park, J., Skrzypek, M. S., … Wong, E. D. (2012). Saccharomyces Genome Database: The genomics resource of budding yeast. Nucleic Acids Research, 40(D1), 700–705. https://doi.org/10.1093/nar/gkr1029

Cid, V. J., Shulewitz, M. J., McDonald, K. L., & Thorner, J. (2001). Dynamic localization of the Swe1 regulator Hsl7 during the *Saccharomyces cerevisiae* cell cycle. Molecular Biology of the Cell, 12(6), 1645–1669. https://doi.org/10.1091/mbc.12.6.1645

Clotet, J., Escoté, X., Adrover, M. Á., Yaakov, G., Garí, E., Aldea, M., De Nadal, E., & Posas, F. (2006). Phosphorylation of Hsl1 by Hog1 leads to a G2 arrest essential for cell survival at high osmolarity. EMBO Journal, 25(11), 2338–2346. https://doi.org/10.1038/sj.emboj.7601095

Crosbie, P. A. J., Crosbie, E. J., Aspinall-O'Dea, M., Walker, M., Harrison, R., Pernemalm, M., Shah, R., Joseph, L., Booton, R., Pierce, A., & Whetton, A. D. (2016). ERK and AKT phosphorylation status in lung cancer and emphysema using nanocapillary isoelectric focusing. BMJ Open Respiratory Research, 3(1). https://doi.org/10.1136/bmjresp-2015-000114

De Nadal, E., Zapater, M., Alepuz, P. M., Sumoy, L., Mas, G., & Posas, F. (2004). The MAPK Hog1 recruits Rpd3 histone deacetylase to activate osmoresponsive genes. Nature, 427(6972), 370–374. https://doi.org/10.1038/nature02258

Eberharter, A., Sterner, D. E., Schieltz, D., Hassan, A., Yates, J. R., Berger, S. L., & Workman, J. L. (1999). The ADA Complex Is a Distinct Histone Acetyltransferase Complex in *Saccharomyces cerevisiae*. Molecular and Cellular Biology, 19(10), 6621–6631. https://doi.org/10.1128/mcb.19.10.6621

Elion, E. A. (2003). MAP Kinase in Yeast. Handbook of Cell Signaling, 2–3, 357–363. https://doi.org/10.1016/B978-012124546-7/50544-1

Eriksson, P. R., Ganguli, D., Nagarajavel, V., & Clark, D. J. (2012). Regulation of histone gene expression in budding yeast. Genetics, 191(1), 7–20. https://doi.org/10.1534/genetics.112.140145

Erkina, T. Y., & Erkine, A. M. (2006). Displacement of Histones at Promoters of *Saccharomyces cerevisiae* Heat Shock Genes Is Differentially Associated with Histone H3 Acetylation. Molecular and Cellular Biology, 26(20), 7587–7600. https://doi.org/10.1128/mcb.00666-06

Escoté, X., Zapater, M., Clotet, J., & Posas, F. (2004). Hog1 mediates cell-cycle arrest in G1 phase by the dual targeting of Sic1. Nature Cell Biology, 6(10), 997–1002. https://doi.org/10.1038/ncb1174

Espinosa, M. C., Rehman, M. A., Chisamore-Robert, P., Jeffery, D., & Yankulov, K. (2010). GCN5 is a positive regulator of origins of DNA replication in *Saccharomyces cerevisiae*. PLoS ONE, 5(1). https://doi.org/10.1371/journal.pone.0008964

Gowans, G. J., Bridgers, J. B., Zhang, J., Dronamraju, R., Burnetti, A., King, D. A., Thiengmany, A. V., Shinsky, S. A., Bhanu, N. V., Garcia, B. A., Buchler, N. E., Strahl, B. D., & Morrison, A. J. (2019). Recognition of Histone Crotonylation by Taf14 Links Metabolic State to Gene Expression. Molecular Cell, 76(6), 909-921.e3. https://doi.org/10.1016/j.molcel.2019.09.029

Grant, P. A., Duggan, L., Côté, J., Roberts, S. M., Brownell, J. E., Candau, R., Ohba, R., Owen-Hughes, T., Allis, C. D., Winston, F., Berger, S. L., & Workman, J. L. (1997). Yeast Gcn5 functions in two multisubunit complexes to acetylate nucleosomal histones: Characterization of an ada complex and the saga (spt/ada) complex. Genes and Development, 11(13), 1640–1650. https://doi.org/10.1101/gad.11.13.1640

Guégan, J.-P., Frémin, C., & Baffet, G. (2012). The MAPK MEK1/2-ERK1/2 Pathway and Its Implication in Hepatocyte Cell Cycle Control. International Journal of Hepatology, 2012, 1–13. https://doi.org/10.1155/2012/328372

Han, Q., Lu, J., Duan, J., Su, D., Hou, X., Li, F., Wang, X., & Huang, B. (2008). Gcn5- and Elp3-induced histone H3 acetylation regulates hsp70 gene transcription in yeast. Biochemical Journal, 409(3), 779–788. https://doi.org/10.1042/BJ20070578

Hartwell, L., & Weinert, T. A. (1989). Checkpoints: Controls That Ensure the Order of Cell Cycle Events. Science, 246(4930), 629–634. https://doi.org/10.1126/science.2683079

Healy, A. M., Zolnierowicz, S., Stapleton, A. E., Goebl, M., DePaoli-Roach, A. A., & Pringle, J. R. (1991). CDC55, a *Saccharomyces cerevisiae* gene involved in cellular morphogenesis: identification, characterization, and homology to the B subunit of mammalian type 2A protein phosphatase. Molecular and Cellular Biology, 11(11), 5767–5780. https://doi.org/10.1128/mcb.11.11.5767

Howe, L., Auston, D., Grant, P., John, S., Cook, R. G., Workman, J. L., & Pillus, L. (2001). Histone H3 specific acetyltransferases are essential for cell cycle progression. Genes and Development, 15(23), 3144–3154. https://doi.org/10.1101/gad.931401

Huisinga, K. L., & Pugh, B. F. (2004). A Genome-Wide Housekeeping Role for TFIID and a Highly Regulated Stress-Related Role for SAGA in *Saccharomyces cerevisiae*. 13(Februrary), 573–585. https://doi.org/10.1016/S1097-2765(04)00087-5

Imoberdorf, R. M., Topalidou, I., & Strubin, M. (2006). A Role for Gcn5-Mediated Global Histone Acetylation in Transcriptional Regulation. Molecular and Cellular Biology, 26(5), 1610–1616. https://doi.org/10.1128/mcb.26.5.1610-1616.2006

Jazwinski, S. M. (2013). The retrograde response: When mitochondrial quality control is not enough. Biochimica et Biophysica Acta - Molecular Cell Research, 1833(2), 400–409. https://doi.org/10.1016/j.bbamcr.2012.02.010

Jiang, Y. (2006). Regulation of the Cell Cycle by Protein Phosphatase 2A in *Saccharomyces cerevisiae*. Microbiology and Molecular Biology Reviews, 70(2), 440–449. https://doi.org/10.1128/mmbr.00049-05

Jiménez, J., Queralt, E., Posas, F., & de Nadal, E. (2020). The regulation of Net1/Cdc14 by the Hog1 MAPK upon osmostress unravels a new mechanism regulating mitosis. Cell Cycle, 19(17), 2105–2118. https://doi.org/10.1080/15384101.2020.1804222

Jin, F., Liu, H., Liang, F., Rizkallah, R., Hurt, M. M., & Wang, Y. (2008). Temporal control of the dephosphorylation of Cdk substrates by mitotic exit pathways in budding yeast. Proceedings of the National Academy of Sciences of the United States of America, 105(42), 16177–16182. https://doi.org/10.1073/pnas.0808719105

Kim, J. J., Lee, S. Y., & Miller, K. M. (2019). Preserving genome integrity and function: the DNA damage response and histone modifications. Critical Reviews in Biochemistry and Molecular Biology, 54(3), 208–241. https://doi.org/10.1080/10409238.2019.1620676

Kollenstart, L., De Groot, A. J. L., Janssen, G. M. C., Cheng, X., Vreeken, K., Martino, F., Côté, J., Van Veelen, P. A., & Van Attikum, H. (2019). Gcn5 and esa1 function as histone crotonyltransferases to regulate crotonylation-dependent

transcription. Journal of Biological Chemistry, 294(52), 20122–20134. https://doi.org/10.1074/jbc.RA119.010302

Koul, H. K., Pal, M., & Koul, S. (2013). Role of p38 MAP Kinase Signal Transduction in Solid Tumors. Genes and Cancer, 4(9–10), 342–359. https://doi.org/10.1177/1947601913507951

Kouzarides, T. (2007). Chromatin Modifications and Their Function. Cell, 128(4), 693–705. https://doi.org/10.1016/j.cell.2007.02.005

Krebs, J. E., Fry, C. J., Samuels, M. L., & Peterson, C. L. (2000). Global role for chromatin remodeling enzymes in mitotic gene expression. Cell, 102(5), 587–598. https://doi.org/10.1016/S0092-8674(00)00081-7

Lee, J., Spector, D., Godon, C., Labarre, J., & Toledano, M. B. (1999). A new antioxidant with alkyl hydroperoxide defense properties in yeast. Journal of Biological Chemistry, 274(8), 4537–4544. https://doi.org/10.1074/jbc.274.8.4537

Lee, K. K., Sardiu, M. E., Swanson, S. K., Gilmore, J. M., Torok, M., Grant, P. A., Florens, L., Workman, J. L., & Washburn, M. P. (2011). Combinatorial depletion analysis to assemble the network architecture of the SAGA and ADA chromatin remodeling complexes. Molecular Systems Biology, 7(503), 1–12. https://doi.org/10.1038/msb.2011.40

Levin, D. E. (2005). Cell Wall Integrity Signaling in *Saccharomyces cerevisiae* . Microbiology and Molecular Biology Reviews, 69(2), 262–291. https://doi.org/10.1128/mmbr.69.2.262-291.2005

Lew, D. J. (2003). The morphogenesis checkpoint: How yeast cells watch their figures. Current Opinion in Cell Biology, 15(6), 648–653. https://doi.org/10.1016/j.ceb.2003.09.001

Lew, D. J., & Reed, S. I. (1993). Morphogenesis in the yeast cell cycle: Regulation by Cdc28 and cyclins. Journal of Cell Biology, 120(6), 1305–1320. https://doi.org/10.1083/jcb.120.6.1305

Li, R., & Murray, A. W. (1991). Feedback control of mitosis in budding yeast. Cell, 66(3), 519–531. https://doi.org/10.1016/0092-8674(81)90015-5

Liu, D., Vleugel, M., Backer, C. B., Hori, T., Fukagawa, T., Cheeseman, I. M., & Lampson, M. A. (2010). Regulated targeting of protein phosphatase 1 to the outer kinetochore by KNL1 opposes Aurora B kinase. Journal of Cell Biology, 188(6), 809–820. https://doi.org/10.1083/jcb.201001006

Liu, G., Zheng, X., Guan, H., Cao, Y., Qu, H., Kang, J., Ren, X., Lei, J., Dong, M. Q., Li, X., & Li, H. (2019). Architecture of *Saccharomyces cerevisiae* SAGA complex. Cell Discovery, 5(1). https://doi.org/10.1038/s41421-019-0094-x

Lo, W. S., Trievel, R. C., Rojas, J. R., Duggan, L., Hsu, J. Y., Allis, C. D., Marmorstein, R., & Berger, S. L. (2000). Phosphorylation of serine 10 in histone H3 is functionally linked in vitro and in vivo to Gcn5-mediated acetylation at lysine 14. Molecular Cell, 5(6), 917–926. https://doi.org/10.1016/s1097-2765(00)80257-9

Maayan, I., Beenstock, J., Marbach, I., Tabachnick, S., Livnah, O., & Engelberg, D. (2012). Osmostress Induces Autophosphorylation of Hog1 via a C-Terminal Regulatory Region That Is Conserved in p38α. PLoS ONE, 7(9), 1–12. https://doi.org/10.1371/journal.pone.0044749

Maeda, T., Takekawa, M., & Saito, H. (1995). Activation of yeast PBS2 MAPKK by MAPKKKs or by binding of an SH3-containing osmosensor. Science (New York, N.Y.), 269(5223), 554–558. https://doi.org/10.1126/science.7624781

Magraner-Pardo, L., Pelechano, V., Coloma, M. D., & Tordera, V. (2014). Dynamic remodeling of histone modifications in response to osmotic stress in *Saccharomyces cerevisiae*. BMC Genomics, 15(1). https://doi.org/10.1186/1471-2164-15-247

Majaz, S., Tong, Z., Peng, K., Wang, W., Ren, W., Li, M., Liu, K., Mo, P., Li, W., & Yu, C. (2016). Histone acetyl transferase GCN5 promotes human hepatocellular carcinoma progression by enhancing AIB1 expression. Cell and Bioscience, 6(1), 1–11. https://doi.org/10.1186/s13578-016-0114-6

McMillan, J. N., Longtine, M. S., Sia, R. A. L., Theesfeld, C. L., Bardes, E. S. G., Pringle, J. R., & Lew, D. J. (1999). The Morphogenesis Checkpoint in *Saccharomyces cerevisiae* : Cell Cycle Control of Swe1p Degradation by Hsl1p and Hsl7p . Molecular and Cellular Biology, 19(10), 6929–6939. https://doi.org/10.1128/mcb.19.10.6929

McMurray, M. A., Bertin, A., Garcia, G., Lam, L., Nogales, E., & Thorner, J. (2011). Septin Filament Formation Is Essential in Budding Yeast. Developmental Cell, 20(4), 540–549. https://doi.org/10.1016/j.devcel.2011.02.004

Meluh, P. B., Yang, P., Glowczewski, L., Koshland, D., & Smith, M. M. (1998). Cse4p is a component of the core centromere of *Saccharomyces cerevisiae*. Cell, 94(5), 607–613. https://doi.org/10.1016/S0092-8674(00)81602-5

Mendenhall, M. D., & Hodge, A. E. (1998). Regulation of Cdc28 Cyclin-Dependent Protein Kinase Activity during the Cell Cycle of the Yeast *Saccharomyces cerevisiae*. Microbiology and Molecular Biology Reviews, 62(4), 1191–1243. https://doi.org/10.1128/mmbr.62.4.1191-1243.1998

Mok, J., Kim, P. M., Lam, H. Y. K., Piccirillo, S., Zhou, X., Jeschke, G. R., Sheridan, D. L., Parker, S. A., Desai, V., Jwa, M., Cameroni, E., Niu, H., Good, M., Remenyi, A., Ma, J.-L. N., Sheu, Y.-J., Sassi, H. E., Sopko, R., Chan, C. S. M., … Turk, B. E. (2010). Deciphering protein kinase specificity through large-scale analysis of yeast phosphorylation site motifs. Science Signaling, 3(109), ra12. https://doi.org/10.1126/scisignal.2000482

Mok, J., Zhu, X., & Snyder, M. (2011). Dissecting phosphorylation networks: Lessons learned from yeast. Expert Review of Proteomics, 8(6), 775–786. https://doi.org/10.1586/epr.11.64

Morillon, A., Springer, M., & Lesage, P. (2000). Activation of the Kss1 Invasive-Filamentous Growth Pathway Induces Ty1 Transcription and Retrotransposition

in *Saccharomyces cerevisiae*. Molecular and Cellular Biology, 20(15), 5766–5776. https://doi.org/10.1128/mcb.20.15.5766-5776.2000

Mustachio, L. M., Roszik, J., Farria, A. T., Guerra, K., & Dent, S. Y. (2019). Repression of GCN5 expression or activity attenuates c-MYC expression in non-small cell lung cancer. American Journal of Cancer Research, 9(8), 1830–1845. http://www.ncbi.nlm.nih.gov/pubmed/31497362%0Ahttp://www.pubmedcentral.nih.gov/articlerender.fcgi?artid=PMC6726999

Nagy, Z., & Tora, L. (2007). Distinct GCN5/PCAF-containing complexes function as co-activators and are involved in transcription factor and global histone acetylation. Oncogene, 26(37), 5341–5357. https://doi.org/10.1038/sj.onc.1210604

Nerusheva, O. O., Galander, S., Fernius, J., Kelly, D., & Marston, A. L. (2014). Tension-dependent removal of pericentromeric shugoshin is an indicator of sister chromosome biorientation. Genes and Development, 28(12), 1291–1309. https://doi.org/10.1101/gad.240291.114

O'Rourke, S. M., & Herskowitz, I. (2002). A Third Osmosensing Branch in *Saccharomyces cerevisiae* Requires the Msb2 Protein and Functions in Parallel with the Sho1 Branch . Molecular and Cellular Biology, 22(13), 4739–4749. https://doi.org/10.1128/mcb.22.13.4739-4749.2002

Pai, C. C., Deegan, R. S., Subramanian, L., Gal, C., Sarkar, S., Blaikley, E. J., Walker, C., Hulme, L., Bernhard, E., Codlin, S., Bähler, J., Allshire, R., Whitehall, S., & Humphrey, T. C. (2014). A histone H3K36 chromatin switch coordinates DNA double-strand break repair pathway choice. Nature Communications, 5(May). https://doi.org/10.1038/ncomms5091

Peplowska, K., Wallek, A. U., & Storchova, Z. (2014). Sgo1 Regulates Both Condensin and Ipl1/Aurora B to Promote Chromosome Biorientation. PLoS Genetics, 10(6). https://doi.org/10.1371/journal.pgen.1004411

Perrotti, D., & Neviani, P. (2013). Protein phosphatase 2A: A target for anticancer therapy. The Lancet Oncology, 14(6), e229–e238. https://doi.org/10.1016/S1470-2045(12)70558-2

Petty, E. L., Evpak, M., & Pillus, L. (2018). Connecting GCN5's centromeric SAGA to the mitotic tension-sensing checkpoint. Molecular Biology of the Cell, 29(18), 2201–2212. https://doi.org/10.1091/mbc.E17-12-0701

Petty, E. L., Lafon, A., Tomlinson, S. L., Mendelsohn, B. A., & Pillus, L. (2016). Promotion of cell viability and histone gene expression by the acetyltransferase Gcn5 and the protein phosphatase PP2A in *Saccharomyces cerevisiae*. In Genetics (Vol. 203, Issue 4). https://doi.org/10.1534/genetics.116.189506

Pigula, A., Drubin, D. G., & Barnes, G. (2014). Regulation of mitotic spindle disassembly by an environmental stress-sensing pathway in budding yeast. Genetics, 198(3), 1043–1057. https://doi.org/10.1534/genetics.114.163238

Posas, F., Wurgler-Murphy, S. M., Maeda, T., Witten, E. A., Thai, T. C., & Saito, H. (1996). Yeast HOG1 MAP kinase cascade is regulated by a multistep phosphorelay mechanism in the SLN1-YPD1-SSK1 "two-component"

osmosensor. Cell, 86(6), 865–875. https://doi.org/10.1016/s0092-8674(00)80162-2

Raitt, D. C., Posas, F., & Saito, H. (2000). Yeast Cdc42 GTPase and Ste20 PAK-like kinase regulate Sho1-dependent activation of the Hog1 MAPK pathway. EMBO Journal, 19(17), 4623–4631. https://doi.org/10.1093/emboj/19.17.4623

Randhawa, H., Kibble, K., Zeng, H., Moyer, M. P., & Reindl, K. M. (2013). Activation of ERK signaling and induction of colon cancer cell death by piperlongumine. Toxicology in Vitro, 27(6), 1626–1633. https://doi.org/10.1016/j.tiv.2013.04.006

Reiser, V., D'Aquino, K. E., Ee, L.-S., & Amon, A. (2006). The stress-activated mitogen-activated protein kinase signaling cascade promotes exit from mitosis. Molecular Biology of the Cell, 17(7), 3136–3146. https://doi.org/10.1091/mbc.e05-12-1102

Rep, M., Proft, M., Remize, F., Tamás, M., Serrano, R., Thevelein, J. M., & Hohmann, S. (2001). The *Saccharomyces cerevisiae* Sko1p transcription factor mediates HOG pathway-dependent osmotic regulation of a set of genes encoding enzymes implicated in protection from oxidative damage. Molecular Microbiology, 40(5), 1067–1083. https://doi.org/10.1046/j.1365-2958.2001.02384.x

Rossetto, D., Avvakumov, N., & Côté, J. (2012). Histone phosphorylation. Epigenetics, 7(10), 1098–1108. https://doi.org/10.4161/epi.21975

Rubenstein, E. M., & Schmidt, M. C. (2007). Mechanisms regulating the protein kinases of *Saccharomyces cerevisiae*. Eukaryotic Cell, 6(4), 571–583. https://doi.org/10.1128/EC.00026-07

Sanz, A. B., García, R., Rodríguez-Peña, J. M., Nombela, C., & Arroyo, J. (2016). Cooperation between SAGA and SWI/SNF complexes is required for efficient transcriptional responses regulated by the yeast MAPK Slt2. Nucleic Acids Research, 44(15), 7159–7172. https://doi.org/10.1093/nar/gkw324

Shu, Y., Yang, H., Hallberg, E., & Hallberg, R. (1997). Molecular genetic analysis of Rts1p, a B' regulatory subunit of *Saccharomyces cerevisiae* protein phosphatase 2A. Molecular and Cellular Biology, 17(6), 3242–3253. https://doi.org/10.1128/mcb.17.6.3242

Shulewitz, M. J., Inouye, C. J., & Thorner, J. (1999). Hsl7 Localizes to a Septin Ring and Serves as an Adapter in a Regulatory Pathway That Relieves Tyrosine Phosphorylation of Cdc28 Protein Kinase in *Saccharomyces cerevisiae* . Molecular and Cellular Biology, 19(10), 7123–7137. https://doi.org/10.1128/mcb.19.10.7123

Sneddon, A. A., Cohen, P. T., & Stark, M. J. (1990). *Saccharomyces cerevisiae* protein phosphatase 2A performs an essential cellular function and is encoded by two genes. The EMBO Journal, 9(13), 4339–4346. https://doi.org/10.1002/j.1460-2075.1990.tb07883.x

Sparks, J. W., & Brautigan, D. L. (1986). Molecular basis for substrate specificity of protein kinases and phosphatases. International Journal of Biochemistry, 18(6), 497–504. https://doi.org/10.1016/0020-711X(86)90159-X

Srivas, R., Shen, J. P., Yang, C. C., Sun, S. M., Li, J., Gross, A. M., Jensen, J., Licon, K., Bojorquez-Gomez, A., Klepper, K., Huang, J., Pekin, D., Xu, J. L., Yeerna, H., Sivaganesh, V., Kollenstart, L., van Attikum, H., Aza-Blanc, P., Sobol, R. W., & Ideker, T. (2016). A Network of Conserved Synthetic Lethal Interactions for Exploration of Precision Cancer Therapy. Molecular Cell, 63(3), 514–525. https://doi.org/10.1016/j.molcel.2016.06.022

Sterner, D. E., Belotserkovskaya, R., & Berger, S. L. (2002). SALSA, a variant of yeast SAGA, contains truncated Spt7, which correlates with activated transcription. Proceedings of the National Academy of Sciences of the United States of America, 99(18), 11622–11627. https://doi.org/10.1073/pnas.182021199

Tamburini, B. A., & Tyler, J. K. (2005). Localized Histone Acetylation and Deacetylation Triggered by the Homologous Recombination Pathway of Double-Strand DNA Repair. Molecular and Cellular Biology, 25(12), 4903–4913. https://doi.org/10.1128/mcb.25.12.4903-4913.2005

Tognetti, S., Jiménez, J., Viganò, M., Duch, A., Queralt, E., de Nadal, E., & Posas, F. (2020). Hog1 activation delays mitotic exit via phosphorylation of Net1. Proceedings of the National Academy of Sciences of the United States of America, 117(16), 8924–8933. https://doi.org/10.1073/pnas.1918308117

van Zyl, W., Huang, W., Sneddon, A. A., Stark, M., Camier, S., Werner, M., Marck, C., Sentenac, A., & Broach, J. R. (1992). Inactivation of the protein phosphatase 2A regulatory subunit A results in morphological and transcriptional defects in *Saccharomyces cerevisiae*. Molecular and Cellular Biology, 12(11), 4946–4959. https://doi.org/10.1128/mcb.12.11.4946

Vasquez, R. J., Howell, B., Yvon, A. M. C., Wadsworth, P., & Cassimeris, L. (1997). Nanomolar concentrations of nocodazole alter microtubule dynamic instability in vivo and in vitro. Molecular Biology of the Cell, 8(6), 973–985. https://doi.org/10.1091/mbc.8.6.973

Viéitez, C., Martínez-Cebrián, G., Solé, C., Böttcher, R., Potel, C. M., Savitski, M. M., Onnebo, S., Fabregat, M., Shilatifard, A., Posas, F., & de Nadal, E. (2020). A genetic analysis reveals novel histone residues required for transcriptional reprogramming upon stress. Nucleic Acids Research, 48(7), 3455–3475. https://doi.org/10.1093/NAR/GKAA081

Visintin, R., Craig, K., Hwang, E. S., Prinz, S., Tyers, M., & Amon, A. (1998). The phosphatase Cdc14 triggers mitotic exit by reversal of Cdk-dependent phosphorylation. Molecular Cell, 2(6), 709–718. https://doi.org/10.1016/S1097-2765(00)80286-5

Wang, C., Xu, H., Lin, S., Deng, W., Zhou, J., Zhang, Y., Shi, Y., Peng, D., & Xue, Y. (2020). GPS 5.0: An Update on the Prediction of Kinase-specific Phosphorylation Sites in Proteins. Genomics, Proteomics and Bioinformatics, 18(1), 72–80. https://doi.org/10.1016/j.gpb.2020.01.001

Wang, S. N., Lee, K. T., Tsai, C. J., Chen, Y. J., & Yeh, Y. T. (2012). Phosphorylated p38 and JNK MAPK proteins in hepatocellular carcinoma. European Journal of Clinical Investigation, 42(12), 1295–1301. https://doi.org/10.1111/eci.12003

Wang, Y., & Burke, D. J. (1995). Checkpoint genes required to delay cell division in response to nocodazole respond to impaired kinetochore function in the yeast *Saccharomyces cerevisiae*. Molecular and Cellular Biology, 15(12), 6838–6844. https://doi.org/10.1128/mcb.15.12.6838

Wyatt, M. D., & Pittman, D. L. (2006). Methylating agents and DNA repair responses: Methylated bases and sources of strand breaks. Chemical Research in Toxicology, 19(12), 1580–1594. https://doi.org/10.1021/tx060164e

Wyce, A., Xiao, T., Whelan, K. A., Kosman, C., Walter, W., Eick, D., Hughes, T. R., Krogan, N. J., Strahl, B. D., & Berger, S. L. (2007). H2B Ubiquitylation Acts as a Barrier to Ctk1 Nucleosomal Recruitment Prior to Removal by Ubp8 within a SAGA-Related Complex. Molecular Cell, 27(2), 275–288. https://doi.org/10.1016/j.molcel.2007.01.035

Xue-Franzén, Y., Henriksson, J., Bürglin, T. R., & Wright, A. P. H. (2013). Distinct roles of the Gcn5 histone acetyltransferase revealed during transient stress-induced reprogramming of the genome. BMC Genomics, 14(1). https://doi.org/10.1186/1471-2164-14-479

Xue-Franzén, Y., Johnsson, A., Brodin, D., Henriksson, J., Bürglin, T. R., & Wright, A. P. H. (2010). Genome-wide characterisation of the Gcn5 histone acetyltransferase in budding yeast during stress adaptation reveals evolutionarily conserved and diverged roles. BMC Genomics, 11(1). https://doi.org/10.1186/1471-2164-11-200

Yaakov, G., Duch, A., García-Rubio, M., Clotet, J., Jimenez, J., Aguilera, A., & Posas, F. (2009). The stress-activated protein kinase Hog1 mediates S phase delay in response to osmostress. Molecular Biology of the Cell, 20(15), 3572–3582. https://doi.org/10.1091/mbc.e09-02-0129

Yang, S. Y., Miah, A., Sales, K. M., Fuller, B., Seifalian, A. M., & Winslet, M. (2011). Inhibition of the p38 MAPK pathway sensitises human colon cancer cells to 5-fluorouracil treatment. International Journal of Oncology, 38(6), 1695–1702. https://doi.org/10.3892/ijo.2011.982

Yin, Y. W., Jin, H. J., Zhao, W., Gao, B., Fang, J., Wei, J., Zhang, D. D., Zhang, J., & Fang, D. (2015). The histone acetyltransferase GCN5 expression is elevated and regulated by c-Myc and E2F1 transcription factors in human colon cancer. Gene Expression, 16(4), 187–196. https://doi.org/10.3727/105221615X14399878166230

Zheng, M., Liu, X., Lin, J., Liu, X., Wang, Z., Xin, M., Yao, Y., Peng, H., Zhou, D. X., Ni, Z., Sun, Q., & Hu, Z. (2019). Histone acetyltransferase GCN5 contributes to cell wall integrity and salt stress tolerance by altering the expression of cellulose synthesis genes. Plant Journal, 97(3), 587–602. https://doi.org/10.1111/tpj.14144